Assessing Selected Technologies and Operational Strategies for Improving the Environmental Performance of Future Aircraft

by

Anuja Mahashabde

B.S. Mechanical Engineering
Rutgers University, 2004

Submitted to the Department of Aeronautics and Astronautics
in partial fulfillment of the requirements for the degree of

Master of Science in Aeronautics and Astronautics

at the

MASSACHUSETTS INSTITUTE OF TECHNOLOGY

June 2006

Author .....
Department of Aeronautics and Astronautics
May 26, 2006

Certified by .....
Ian A. Waitz
Professor of Aeronautics and Astronautics
Thesis Supervisor

Accepted by .....
Jaime Peraire
Professor of Aeronautics and Astronautics
Chair, Committee on Graduate Students

Assessing Selected Technologies and Operational Strategies for Improving the Environmental Performance of Future Aircraft

by

Anuja Mahashabde

Submitted to the Department of Aeronautics and Astronautics
on May 26, 2006, in partial fulfillment of the
requirements for the degree of
Master of Science in Aeronautics and Astronautics

Abstract

The aviation industry is expected to grow at a rate of 4-5% in the next 20 years. Such a growth rate may have important impacts on local air quality, climate change and community noise. This work assesses selected technologies and operational procedures aimed at improving the environmental performance of future airplanes.

Two different studies are presented: estimating turbine durability benefits from jet engine water injection and evaluating improvements in fuel burn and operating costs from using advanced technology, high bypass ratio engines and varying the design cruise speed. Water injection in commercial airplane engine combustors lowers operating temperatures and can lead to significant reductions in NO_x and soot emissions, potentially improving engine hot section life. With increasing fuel prices and possible introduction of emissions trading in the future, fuel burn may become a more critical aircraft design driver. Increasing engine bypass ratio and lowering cruise speed can lead to reduced fuel consumption.

The dominant mechanisms of failure in turbine blades are low cycle fatigue, creep and oxidation. The Universal Slopes method is used to evaluate possible fatigue life benefits from water injection for three representative blade materials. For a 67K change in turbine inlet temperature, metal temperature changes up to 47K are expected. Life improvement with a 47K change in metal temperature is possible up to a factor of 1.90 for Inconel 625, up to 1.46 for Inconel 706 and up to 2.85 for René 80 depending on the strains imposed. Blade life effects of creep and oxidation for varying temperatures are presented based on a literature review. The absolute value of possible benefits strongly depend on material properties, metal and gas temperatures (internal and external to the blade) and stress levels.

In addition, a maintenance cost analysis is performed to evaluate and compare

benefits resulting from engine de-rate and water injection using an engine cycle program (GasTurb) and airline data for a typical 1970's technology mixed flow turbofan engine. A 67K change in T_{t4} from water injection corresponds to an average de-rate value of 8.4%. Material maintenance costs in 2004 dollars are reduced by 16.52% to 2.86% for a 1-hour and 12-hour flight length respectively. Results show that shorter range flights, with more takeoffs per day, experience larger benefits.

Engine durability analysis capabilities of a numerical simulation design tool - the Environmental Design Space (EDS) are examined. EDS currently does not have the capability for durability analyses and given the inherent difficulty in finding reliable physics-based models for part life prediction that do not require proprietary data, it seems unlikely that EDS will be able to develop such a capability.

The engine bypass-ratio and cruise speed trade study is conducted for a 737-sized future airplane using Boeing internal tools and data. At higher cruise speeds a clear optimum bypass ratio value for minimizing fuel burn is found; for the UEET engines this optimum BPR is about 14. As cruise speed is lowered, fuel burn continually decreases with increasing bypass ratio for the engines examined. At a fixed bypass ratio, flying slower seems most beneficial for very high fuel prices for minimizing both fuel burn and operating costs.

Thesis Supervisor: Ian A. Waitz
Title: Professor of Aeronautics and Astronautics

Acknowledgments

I would like to start by expressing my gratitude to Prof. Waitz for all his support and guidance throughout the course of this thesis. He has always been a great mentor, actively involved in his students' research efforts. I wish to thank him for his constant encouragement and strong belief in my abilities during all those difficult and frustrating times when it seemed that any progress was very hard to come by. I enjoyed working with him also because I had the freedom to explore and try new things.

I also had the opportunity to work with Prof. Karen Willcox towards the end of my thesis. She is an amazing person to work with, always offering insightful comments and suggestions.

Sean Bradshaw provided a lot of help and guidance early on in my research with the turbine blade life analysis. Thanks Sean, for all the interesting conversions and general graduate school survival tips.

It was a pleasure working with the rest of the EDS team here at MIT. I would like to thank Phil Spindler, Paul Rossetti, Tim Yoder, Doug Allaire, Julien Rojo, Karen Marais and Joe Palladino for offering their help on numerous occasions. I would like to thank Yifang Gong for always making time and offering help with my doubts and questions. I would also like to thank Barbara Lechner for helping out in many ways - academic and personal.

It is also important to mention EDS team members at Georgia Institute of Technology that I worked closely with: Jimmy Tai, Michelle Kirby, Jorge DeLuis and Elena Garcia. Thank you for your help and guidance with all EDS related questions and impromptu yahoo messenger sessions.

I appreciate the great advice and useful insights that Philippa Reed and Prof. Mark Spearing at the University of Southampton provided for the turbine blade life analysis.

Next, I want to mention the preliminary design group at Boeing Commercial Airplanes that I have been working with since last summer. I would especially like to thank Dave Daggett for being my mentor at Boeing and for hosting me there last

summer. I would also like to thank Jim Conlin for helping me with the bypass ratio and cruise speed studies. I have learnt a lot from my experience there. Finally, I would like to thank Mithra Sankrithi for approving my stay at Boeing.

On a personal note, I would like to thank my officemates for all those lunch and coffee breaks and great conversations. I would like to thank the GTL folk - Lori Martinez, late Paul Warren and others for the friendly lab environment and keeping the social hour tradition alive. My close friends here at MIT are my support network and have kept me going through all the tough times. I thank them deeply for always being there and for all the fun times and great memories.

Lastly, I want to thank my parents and my sister. None of this would have been conceivable without their love and faith in me. Thank you for everything.

This research has been possible with funding from the National Science Foundation Fellowship, MIT - Aeronautics and Astronautics Departmental Fellowship and Boeing Commercial Airplanes.

Contents

List of Figures

List of Tables

Nomenclature

α	coefficient of expansion of the blade material $[K^{-1}]$
η_{poly}	Polytropic efficiency
$\frac{L}{D}$	Lift to Drag ratio
$\frac{t}{c}$	Thickness to chord ratio
$\bar{T}$	average material temperature [K]
$\dot{m}$	Mass flow [kg/s]
σ_{th}	Thermal stress [Pa]
a	Speed of sound [mi/hr]
AR	Aspect ratio
b	Basquin exponent
c	Fatigue ductility exponent
C_D	Drag coefficient
C_L	Lift coefficient
C_{Lmax}	Maximum lift coefficient
E	Young's modulus [Pa]
k	Wall thermal conductivity [W/mK]

M	Mach number
N_f	Number of cycles to crack initiation
N_{fmaxT}	Fatigue life at the maximum temperature used
t	Wall thickness [m]
T_{t4}	Turbine inlet temperature [K]
T_{wall}	Blade wall temperature [K]
V_{app}	Approach speed [knots]
W	Airplane gross weight [lbf]
ϵ_e	elastic strain
$\epsilon_f^{'}$	Fatigue ductility coefficient
ϵ_p	plastic strain
ϵ_f	True fracture ductility
Λ	Sweep (°)
$\dot{q}$	Heat transfer rate [W/m^2]
$\sigma_f^{'}$	Fatigue strength coefficient [Pa]
σ_{ult}	Ultimate tensile strength [Pa]
h	Heat transfer coefficient [W/m^{2}K]
RA	Area reduction of stressed component
T_{cool}	Cooling flow gas temperature [K]
T_{gas}	Turbine inlet external gas temperature = T_{t4} [K]
T	Local material temperature [K]

AEDT	Aviation Environmental Design Tool
ALCCA	Aircraft Life-Cycle Cost Analysis Code
ANOPP	Noise Prediction Computer Code for Advanced Subsonic Propulsion Systems
APMT	Aviation Environmental Portfolio Management Tool
ATC	Air Traffic Control
BPR	Bypass Ratio
CAEP	Committee on Aviation Environmental Protection
CAROC	Cash Airplane Related Operating Costs
EDS	Environmental Design Space
FAA	Federal Aviation Administration
FAA-AEE	FAA's Office of Energy and Emissions
FLOPS	Flight Optimization System Aircraft Performance and Sizing Code
ICAO	International Civil Aviation Organization
MMC/EFH	Material Maintenance Costs per Engine Flight Hour [$/hour]
NPSS	Numerical Propulsion System Simulation
OEW	Airplane Operating Empty Weight [lb]
OPR	Overall Pressure Ratio
RDT&E	Research, Development, Testing and Evaluation
SFC	Specific Fuel Consumption [lb/hr/lb]
TBC	Thermal Barrier Coatings

TMF	Thermo-Mechanical Fatigue
TOFL	Takeoff Field Length [ft]
UEET	Ultra-Efficient Engine Technology
WATE	Weight Analysis of Turbine Engines

Chapter 1

Introduction

1.1 Background

Environmental impacts of aviation are becoming increasingly important as the aviation industry is expected to grow at a steady pace. The 2005 Boeing market outlook states an expected global growth rate of 4.8% for passenger traffic and of 6.2% for cargo in the next 20 years [1]. The Federal Aviation Administration (FAA) aerospace forecast also predicts similar industry growth rates of about 4-5% per year [2]. The primary environmental impacts of aviation are on local air quality, global climate and community noise. Exhaust pollutants include CO_2, water vapor, oxides of Nitrogen (NO_x), unburned hydrocarbons (HC), carbon monoxide (CO), and sulfur oxides (SO_x). While reductions in fuel consumption typically also result in emissions reductions, some types of emissions are strongly dependent on engine design parameters. For instance NO_x emissions rely heavily on combustor design details, the actual combustion process and the engine pressure ratio. Thus, there is a need to explore methods for both reducing aircraft fuel burn as well as specifically for lowering emissions.

Historically, it is seen that the fuel efficiency of the U.S. fleet has improved by 60% from 1971 to 1998 owing to both technological and operational changes [3]. Fuel efficiency is expected to improve at a rate of 1-2% per year by 2025 resulting from further airframe and engine improvements [3]. The implementation of such "green" technologies and operations requires a careful analysis of the tradeoffs between con-

siderations like performance, emissions, noise and cost. In terms of environmental objectives, the interdependencies between the different kinds of pollutants and noise have to be properly evaluated through the design process. Additionally, the environmental, operational and economic impacts of different policy scenarios have not be assessed in an all encompassing manner yet. In addressing aviation's impacts on the environment, a two-fold approach is necessary. The first is a need for technologies and operational procedures that mitigate emissions and noise. Secondly, to make such solutions economically viable, they have to be analyzed to understand the interrelations between possibly conflicting performance and economical objectives. For instance, a new technology that reduces fuel burn may be very impractical to implement due to the associated increase in operating costs. This necessitates the use of a numerical simulation airplane design tool that works in conjunction with other modules having the capability of estimating impacts on local air quality, noise and global climate. Finally, the proposed environmentally-friendly airplane designs have to be assessed in terms of social costs and benefits associated with technology or policy scenarios. The development of such design tools is important in aiding policy-making decisions where the impacts of proposed changes can be propagated to fleet level operations [4].

The FAA's Office of Energy and Emissions (FAA-AEE) is currently developing a suite of tools to assess aviation's environmental impacts and the interdependencies between noise, emissions and performance. These tools will provide the capability of including environmental objectives in the design process such as emissions reduction or noise abatement. It is expected that the International Civil Aviation Organization (ICAO), specifically its Committee on Aviation Environmental Protection (CAEP) will be the primary users of these tools. This suite of tools can be broken down to different modules and is broadly divided into three sections. The different modules used within this framework are either existing tools or newly developed modules. The Aviation Environmental Portfolio Management Tool (APMT) is the economic analysis tool and addresses the social costs and benefits associated with environmental policy scenarios. APMT interfaces with two other components: Aviation Environmental Design Tool (AEDT) and the Environmental Design Space (EDS). AEDT takes fleet and

schedule data as inputs and provides local and global emissions inventories and noise data. EDS provides the capability to estimate source noise, emissions, performance and cost parameters for different technological scenarios. High fidelity future airplane design simulation is possible through EDS. APMT, AEDT and EDS work together to analyze various policy and technological scenarios for environmental regulations. Figure 1-1 shows the framework for these modules. For instance, the feasibility of implementing a higher stringency level for NO_x can be tested by imposing it as a constraint in the airplane design in EDS. The tradeoffs between noise, NOx, other emissions, fuel burn and the resulting costs can then be examined in detail for the resulting design as well as for fleet level changes. This data when provided to AEDT gives local and global environmental impacts that are economically and socially quantified through APMT [5].

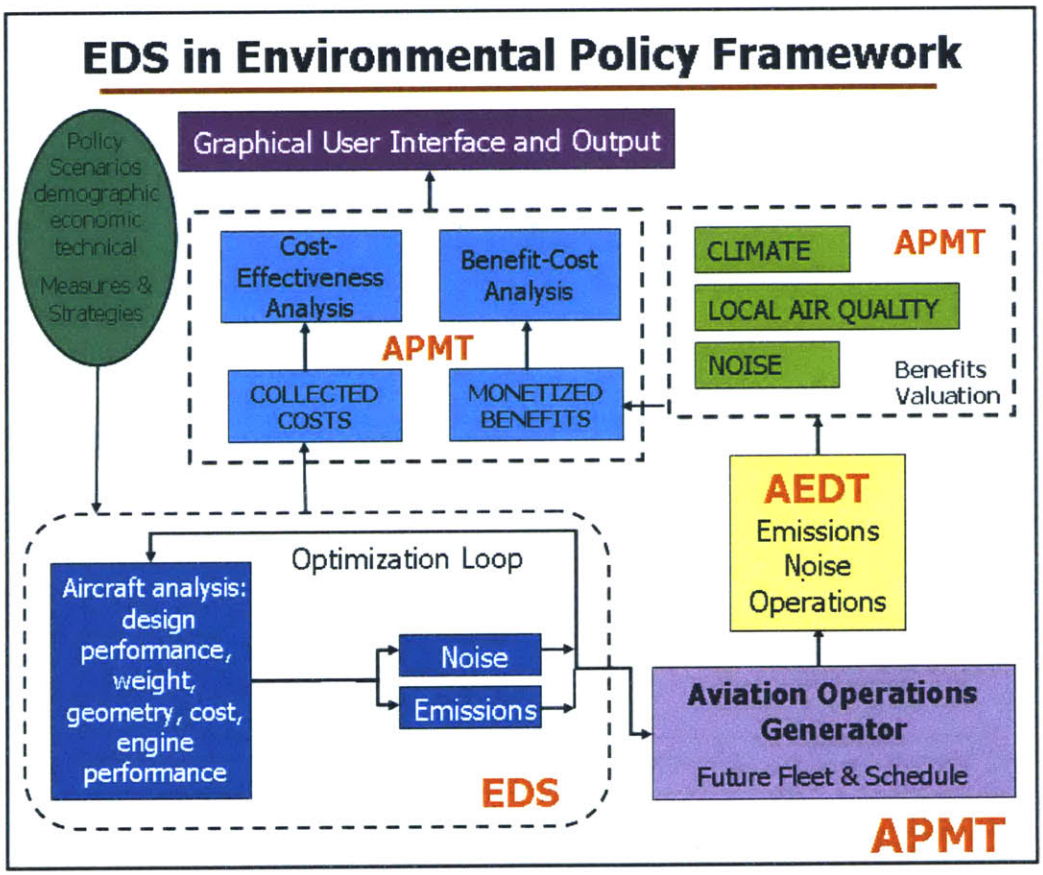

Figure 1-1: APMT, AEDT, EDS framework

The purpose of this thesis is to follow on the two-step process mentioned previously for assessing the environmental impacts of aviation. Two separate studies are presented: turbine durability impacts of jet engine water injection and operator cost sensitivity to cruise speed, engine bypass ratio (BPR) and fuel price.

A Boeing study [6] reveals that NO_x reductions up to 80% are possible during takeoff from water injection. However, this technology involves penalties such as weight increases from carrying water tanks and for implementation purposes other possible benefits need to be examined. Water injection essentially reduces operating temperatures in the engine hot section and thus may increase component part life. Work presented in this thesis examines the potential live savings and maintenance cost benefits possible from water injection.

Another study included in this thesis looks at the tradeoffs involved in varying BPR, cruise speed on the fuel burn of a 737-sized future airplane. With increasing jet fuel prices and possible future environmental levies in the form of emissions trading or taxes, fuel burn is becoming an even more critical consideration in the design process. Figure 1-2 shows the trends in jet fuel prices and aircraft miles traveled per capita from 1994 to 2004 [7]. The jet fuel prices have been adjusted for inflation to 2000 chained dollars [1].

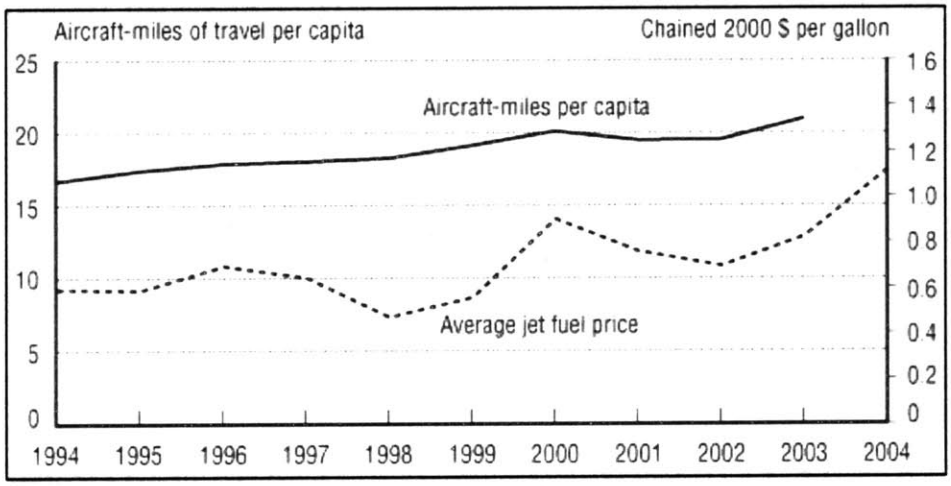

Figure 1-2: U.S. historical trends in jet fuel price [7]

[1]Chained dollars are used to adjust for inflation; the 2000 indices are the most recent values available from the Bureau of Economic Analysis (BEA)

The data shown in Figure 1-2 is based on U.S. refiner prices to end users. Observing from Figure 1-2, jet fuel prices have shown overall steady increases from 1994 to 2004. There is a direct correlation between kilograms of CO_2 produced per kilogram of fuel burnt; for aviation this is valued at 3.16 kg of CO_2 per kg of fuel [8]. CO_2-related emissions costs are used here to demonstrate impacts of possible future environmental costs. Based on current estimates and correcting for 2006 dollars, CO_2 is priced between $8 and $170 per metric tonne [9].

Increasing BPR improves engine specific fuel consumption, however, with increasing BPR weight and drag penalties are also incurred. Selecting an appropriate BPR in airplane design involves a tradeoff between fuel efficiency and weight and drag impacts. Flying at lower cruise speeds may be another means of reducing aircraft fuel burn, provided that the reduction in speed does not greatly increase flight duration to offset fuel burn reductions and all other performance criteria are met. The trade space including engine bypass ratio and cruise speed needs to be explored for possible improvements in fuel burn. More fuel efficient future aircraft will also help in mitigating environmental impacts. Direct operating costs include fuel as well as time related costs. Hence, operating cost sensitivities to changes in BPR and cruise speed under different future fuel price scenarios are also examined. This trade study was conducted using Boeing internal tools and data.

The results from the water injection study are also used specifically to understand the current and future capabilities of the EDS module. Currently, in its initial version, EDS is composed of existing NASA design tools. These are the Numerical Propulsion System Simulation (NPSS), the Weight Analysis of Turbine Engines (WATE) program, the Flight Optimization System Aircraft Performance and Sizing Code (FLOPS), the Noise Prediction Computer Code for Advanced Subsonic Propulsion Systems (ANOPP), and the Aircraft Life-Cycle Cost Analysis Code (ALCCA) [5]. The results from the water injection analysis are used to assess the engine part life prediction capability of EDS; the maintenance cost estimation capabilities of the ALCCA module are also examined. The subsequent sections of this chapter present the organization and key contributions of this thesis.

1.2 Thesis organization

This section provides a brief description of the organization and structure of the different chapters. There are four chapters in this thesis; the contents of each chapter are outlined below.

Chapter 2:

Chapter 2 focuses on water injection technology as a means of reducing NO_x emissions and improving engine hot section life and thus maintenance costs. NO_x reductions of up to 80% and turbine inlet temperature reductions of approximately 67K (120°F) are possible during takeoff when water is sprayed into the engine combustor [6]. This corresponds to metal temperature changes of about 34K-47K. The Universal Slopes method is used to quantify turbine blade fatigue life benefits possible from reduced operating temperatures. A brief discussion of results based on a literature review is also presented for the other principal failure modes - creep and oxidation. Additionally, airline data [11] available on material maintenance costs benefits from takeoff de-rate procedures are used to demonstrate possible maintenance cost benefits from water injection. The results of this study are then applied to understanding current and future capabilities of EDS and ALCCA in predicting engine component life and estimating maintenance costs.

Chapter 3:

Results from the trade study on the effects of cruise speed and BPR on block fuel trends and operating costs for a 737-class airplane are presented in Chapter 3. Escalating fuel prices and possible environmental levies in the future may make fuel burn reduction a key design objective. Lowering cruise speed and increasing engine BPR can be good strategies for improving aircraft fuel efficiency. Boeing internal data and analysis tools are used for the analyses in this chapter. Using some simplifying assumptions, block fuel trends are obtained for varying engines with different BPRs and for different cruise Mach numbers. The block time and block fuel results from these

performance analyses are then used in an operating cost sensitivity study. Variations in operating costs are shown with changing cruise Mach, BPR and fuel prices. Finally, the assumptions used in the study are critically examined and recommendations are provided for future work.

Chapter 4:
Chapter 4 is the concluding chapter of the thesis. This chapter summarizes and highlights important conclusions derived from the work presented in the preceding chapters.

1.3 Key contributions

The work presented in this thesis has a two-fold purpose. The first goal is to assess selected technologies and operational strategies aimed at improving the environmental performance of future aircraft. Secondly, the results from these analyses are used to understand some of the potential capabilities and limitations of specific modules within the Environmental Design Space suite of tools. The main contributions of this thesis are listed below:

- Potential fatigue life benefits resulting from water injection in jet engines are quantified based on an empirical model.
- Turbine inlet temperature reductions from de-rated operations are correlated with temperature changes from water injection to estimate possible maintenance cost benefits resulting from the water injection technology.
- Engine life prediction and maintenance cost estimation capabilities and limitations of the ALCCA module in EDS are identified.
- Block fuel trends are demonstrated for varying BPR and cruise Mach for a 737-sized future airplane using simplifying assumptions.

- Operator cost sensitivity to BPR, cruise speed and fuel price is also explored using the results from the cruise speed-BPR trade study.
- Recommendations are provided for future work in understanding the impacts of cruise speed on airplane fuel efficiency.

Chapter 2

Water injection: Turbine blade life and maintenance cost benefits

Water injection is a well-established technology in the industrial power generation sector and is used for NO_x reduction as well as power augmentation. The implementation of a water injection system in commercial airplane engines may lead to significant reductions in NO_x and soot emissions with possible improvements in the engine hot section life (i.e in the combustor and the turbine). Improvement in the hot section life is anticipated as water injection reduces the operating temperature of the engine components. This chapter focuses on analyzing the effects of water injection specifically on turbine life and on maintenance costs.

For the purposes of this study, it is assumed that turbine life is primarily limited by the temperatures experienced by the blades. The dominant mechanisms of failure in turbine blades are identified as low cycle fatigue, creep and oxidation. Using the Universal Slopes method, a preliminary quantitative analysis of possible fatigue life benefits from water injection has been performed for three representative blade materials, Inconel 625, Inconel 706 and René 80. The selection of these materials for the proposed blade life estimation analysis is largely dependent on data access and availability. Quantitative results are presented only for the fatigue failure mode. A detailed investigation of the combined effects of fatigue, creep and oxidation is not feasible through a generic life model. Consequently, a brief overview of the effects of

creep and oxidation is presented as found in the literature.

In addition, a maintenance cost analysis is performed to evaluate and compare benefits resulting from engine de-rate and water injection. An engine cycle program, GasTurb [10], and airline data [11] are used to correlate changes in turbine inlet temperature and corresponding changes in maintenance costs for a typical 1970's technology mixed flow turbofan engine.

The shortcomings of these studies are also discussed and recommendations for future work are presented. Finally, the implications of the results of this study for modeling capabilities of the Environmental Design Space suite of tools(EDS) are considered. The Aircraft Life Cycle Cost Analysis (ALCCA) module within EDS estimates airplane RDT&E, production and operations costs. The turbine blade life and maintenance cost results are used to briefly discuss the current and potential capabilities of EDS and ALCCA in the area of estimating component life and maintenance costs.

2.1 The Boeing water injection study

In the aviation industry, water injection has been used in the early Boeing 707 and Boeing 747 commercial jet engines for takeoff thrust enhancement; however, current technology jet engines are capable of much higher power production and no longer use water injection for that purpose. Today, the technology holds the potential to improve the turbine blade life in addition to reducing NO_x and soot emissions. Data obtained from Boeing [6] reveals that NO_x reductions of up to 80% are possible during takeoff when water is sprayed into the engine combustor with a water to fuel ratio of 1:1. For a 747-400 size aircraft, an 80% reduction in NO_x may save about 56 lb of emissions. Water injection in the combustor also corresponds to temperature reductions of approximately 67K (120°F) in the turbine inlet.

The Boeing study was conducted to assess the implementation potential of the water injection technology on a Boeing 747-400 airplane to reduce NO_x emissions during takeoff. 400 gallons of conditioned water would have to be carried on board

for use during takeoff upto 3000 ft. This resulted in a weight penalty of about 4,090 lb from carrying the water and necessary system equipment that could reduce aircraft range and increase mission fuel required. Water injection also tends to reduced compressor stall margins and overcoming this problem may incur fuel efficiency penalties. It was found that retrofitting existing aircraft with this technology would be too cost intensive. The implementation of water injection technology would only benefit newly designed airplanes as the required system changes could be incorporated in the design process [6].

The benefits offered by water injection - takeoff NO_x reduction and potential engine hot-section maintenance cost improvements may be able to offset other weight and operational penalties encountered. NO_x reductions could help save in operating costs at airports where emissions-based charges are imposed. Temperature reductions in the engine hot-section may help by extending part life and lowering maintenance costs. The study presented in this chapter assesses the potential turbine life benefits resulting from water injection to further understand the implementation feasibility of the technology.

2.2 Turbine blade life

The Boeing study estimates changes in turbine inlet gas temperature, T_{t4} to be 67K due to water injection in the combustor. A thermal effect of this magnitude during the critical takeoff portion of the mission can have significant impacts on the turbine blade life. External gas temperature reductions in the turbine do not directly translate to equivalent reductions in blade metal temperature, T_{wall}. In this study it is assumed that ΔT_{wall} ranges from 50% to 70% of ΔT_{t4}. This assumption is based on personal communication with Boeing and data published in the Boeing contractor report to NASA on water injection [12]. For a 67K change in T_{t4}, metal temperature changes would range from 34K to 47K. For this study a range of possible life estimates is presented; more accurate results can be obtained with a first order blade heat transfer analysis. Appendix B demonstrates this blade heat transfer analysis and indicates

the data necessary to evaluate changes in blade temperature.

Turbine blade material properties and thermal loads vary greatly with operating temperatures. Life benefits due to water injection are expressed in terms of general trends observed in the predicted life as a function of metal temperature. The results developed are not limited to a particular type of engine or other design details such as blade geometry, but are representative and determined using generic test specimen data sets, not accounting for blade coatings. Fatigue, resulting from cyclic loading on the components, creep and oxidation are known to be dominant failure mechanisms in the engine hot section. Specifically, turbine blades are subjected to high centrifugal stress levels and aerodynamic loadings at elevated temperatures in a corrosive environment. Degradation of turbine blades thus results from a combination of cyclic high stress levels, creep effects from exposure to elevated temperatures as well as environmental factors. Owing to the complexity of the interactions between the different failure mechanisms and the lack of detailed knowledge about the loads and temperatures involved, a high fidelity, physics-based, life prediction model is not feasible. Hence, this chapter investigates fatigue life dependence on temperature through a generalized empirical model. The effects of creep and oxidation on component life are presented as found in the literature for a different set of nickel-base alloys.

2.2.1 Fatigue

Critical cyclic stress imposed for a short duration of time such as takeoff is referred to as low cycle fatigue. Fatigue life characterization is commonly done through total life approaches, where life is divided into two distinct regimes: crack initiation and crack propagation [13]. Total life approaches are based on stress levels or strain levels usually predicting life up to crack initiation and then the propagation life to a critical crack size that is designated as failure. Depending on the operating conditions and loads imposed on the part, the total life of the part is divided between these two regimes.

2.2.1.1 Crack initiation life

In the case of low cycle fatigue at elevated temperatures, material behavior is not purely in the elastic range. Under such circumstances, fatigue life is characterized in terms of the total strain range that the part is subjected to [13]. The total strain amplitude is divided into its elastic and plastic strain amplitudes given by:

$$\frac{\Delta\epsilon}{2} = \frac{\Delta\epsilon_e}{2} + \frac{\Delta\epsilon_p}{2} \tag{2.1}$$

where:

ϵ_e = elastic strain

ϵ_p = plastic strain

Based on log-log plots of experimental data in terms of cycles to failure versus stress levels , the elastic strain can be expressed through the Basquin equation [13] as:

$$\frac{\Delta\epsilon_e}{2} = \frac{\sigma_f^{'}}{E}(2N_f)^b \tag{2.2}$$

where:

E = Young's modulus [Pa]

$\sigma_f^{'}$ = fatigue strength coefficient [Pa]

b = fatigue strength or the Basquin exponent (ranging from -0.05 to -0.12)

N_f = number of cycles to crack initiation

Similarly, according to the Coffin-Manson relation [13], the plastic strain component is expressed as:

$$\frac{\Delta\epsilon_p}{2} = \epsilon_f^{'}(2N_f)^c \tag{2.3}$$

where:

$\epsilon_f^{'}$ = fatigue ductility coefficient

c = fatigue ductility exponent (ranging from -0.5 to -0.7)

Combining equations (2.2) and (2.3) and substituting into equation (2.1) gives:

$$\frac{\Delta\epsilon_{total}}{2} = \frac{\sigma_f^{'}}{E}(2N_f)^b + \epsilon_f^{'}(2N_f)^c \tag{2.4}$$

2.2.1.2 Universal Slopes Method

Although the Coffin-Manson relation was developed for crack initiation life, Manson [14] shows that this relation can be used to predict life up to failure or specimen separation. Based on experimental results obtained from 29 specimens, his results propose a modified version of equation (2.4) for fatigue life prediction. This method is commonly known as the Universal Slopes method and is given by:

$$\Delta\epsilon_{total} = 3.5\frac{\sigma_{ult}}{E}(N_f)^{-0.12} + \epsilon_f^{0.6}(N_f)^{-0.6} \tag{2.5}$$

where:

σ_{ult} = ultimate tensile strength [Pa]

ϵ_f = true fracture ductility (from monotonic tensile tests)

ϵ_f = $\ln(1 + \%\text{elongation})$ or $\epsilon_f = \ln(\frac{1}{1-RA})$

RA = area reduction of stressed component (test specimen)

This method puts forth average values for the exponents in equation (2.4), based on experimental results. These exponent values are not specific to any material and can be used in a preliminary design stage analysis. From equation (2.5) it can be seen that at constant strain, increasing σ_{ult} and ϵ_f and decreasing E enhances material life. Fatigue life degrades with increasing strain. In the Manson study [14], 99.5% of the experimental life data falls within a factor of 20 of the predicted life. For the analysis herein, nickel-base superalloy turbine blade materials, Inconel 625,

Inconel 706 and René 80 are used where the materials properties are obtained from the technical library from High Temp Metals Inc. [15], the Military Handbook [16] and the Aerospace Structural Metals Handbook [17]. The damped Newton-Rhapson method is used to solve equation (2.5) for N_f.

(i) Elastic life:

If only the elastic portion of the Universal Slopes method is used, the life estimate can be solved as:

$$N_f = \left(\frac{\Delta\epsilon_{total} E}{3.5\sigma_{ult}} \right)^{-\frac{1}{0.12}} \tag{2.6a}$$

The elastic life estimate is determined by the ratio of temperature dependent material properties and the strain value.

(ii) Plastic life:

Similarly, if only the plastic part of the method is used, the life is evaluated as:

$$N_f = \epsilon_f (\Delta\epsilon_{total})^{-\frac{1}{0.6}} \tag{2.6b}$$

Here, the plastic life estimate is only a function of ductility, which depends on material temperature, and of the strain value used.

2.2.1.3 Stress level estimation

In order to obtain life estimates from the Universal Slopes method, the total strain range imposed on the blade needs to be approximated. The analysis is performed in two ways: first by keeping the strain level constant and varying temperature dependent material properties and then by varying the strain level as well as material properties with temperature.

(i) Constant strain range estimation:

For the analysis, it is desirable to observe the effects of total strain levels on the life

estimates. The total strain is selected such that the respective stress value is limited at 40% to 80% of the ultimate tensile strength at a given temperature level. This corresponds to applying a design factor of safety of 2.5 to 1.25 respectively. The life cycles to failure are then acquired from equation (2.5), keeping the strain level constant and varying material properties due to temperature changes.

(ii) Temperature-dependent strain range:

It can be expected that as the operating temperature of the blade increases, the thermal stress level increases and there are variations in the total strain as well. These strain variations are expressed through thermal stresses only. This represents in-phase thermo-mechanical loading where the thermal and mechanical loads on the part are increased or decreased simultaneously. Since the centrifugal stresses are not calculated, the thermal stress levels are permitted to be higher than expected such that the total stress level is within a factor of safety of 1.25 to 2.5 of the ultimate strength.

(iii) Thermal stress:

The thermal stress is given by:

$$\sigma_{th} = \alpha E(T - \bar{T}) \tag{2.7}$$

where:

σ_{th} = thermal stress [Pa]
α = coefficient of expansion of the blade material $[K^{-1}]$
T = local material temperature [K]
$\bar{T}$ = average material temperature [K]

Thermal stresses arise from local temperature gradients that cause non-uniform expansion resulting in stresses in the blade.

2.2.1.4 Fatigue life estimate

The Universal Slopes method, as described previously, is used to estimate low cycle fatigue life for turbine blades. Owing to a lack of detailed information about the component geometry, loads and operating conditions, the life prediction methodology selected is based primarily on temperature dependent material behavior. Three different representative alloys are selected for this analysis. Figure 2-1 compares the relevant mechanical properties of these materials [15, 16, 17].

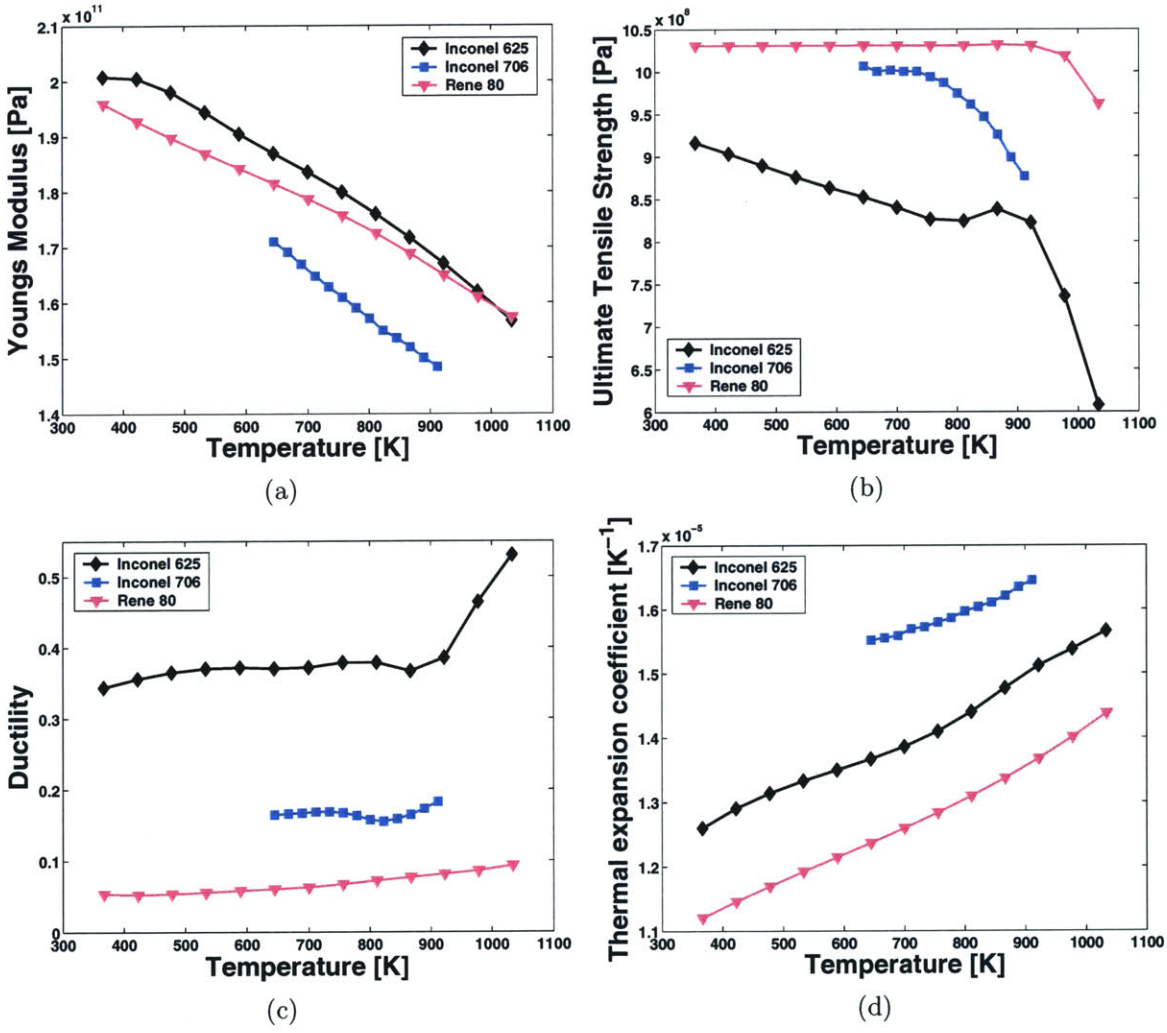

Figure 2-1: Variation in mechanical properties with temperature [15, 16, 17]. Key properties are: (a) Young's modulus, (b) Ultimate tensile strength, (c) Ductility, (d) Thermal expansion coefficient

These material properties show similar general trends for varying metal tempera-

ture levels with differences in magnitudes and it is expected that this will be reflected in the life estimates obtained.

(i) Inconel 625:

Fatigue life predicted by the Universal Slopes method varies greatly depending on several factors such as the material used, whether the elastic or plastic portion of the equation is used, the strain levels, strain dependence on metal temperature and so on. It is important to note again, that the total strain levels selected for the analysis were based on stress levels limited to 40% to 80% of the ultimate strength of the material at the given temperature. A lower range of strain levels for the given temperature reduction would have shown higher life benefits, while a higher strain level would give comparatively lower life benefits. Some of these effects are illustrated in the following discussion for Inconel 625.

For Inconel 625, the elastic and plastic parts of the Universal Slopes method are isolated and life is determined for each type of deformation. This is done using constant strain values as well as with temperature dependent strain. Figure 2-1 compares the elastic life prediction based on how the strain range is defined. Results are plotted as a ratio of fatigue life at a given temperature, N_f, to fatigue life at the maximum temperature used in the analysis, N_{fmaxT} , for the different strain levels versus metal temperature.

Both plots are subject to similar strain ranges, but in Figure 2-2a the strain is held constant while material properties are varied with temperature. From equation (2.6a) it is seen that life is function of material property ratios and the imposed strain. At constant strain values, ratio of N_f at a given temperature to N_{fmaxT} just becomes a ratio of material properties with the strain terms canceling. As a result, all the life ratio curves for the different strains used are identical. For Figure 2-2b, the life ratios are different since the strain values vary with temperature, but the differences are not significant.

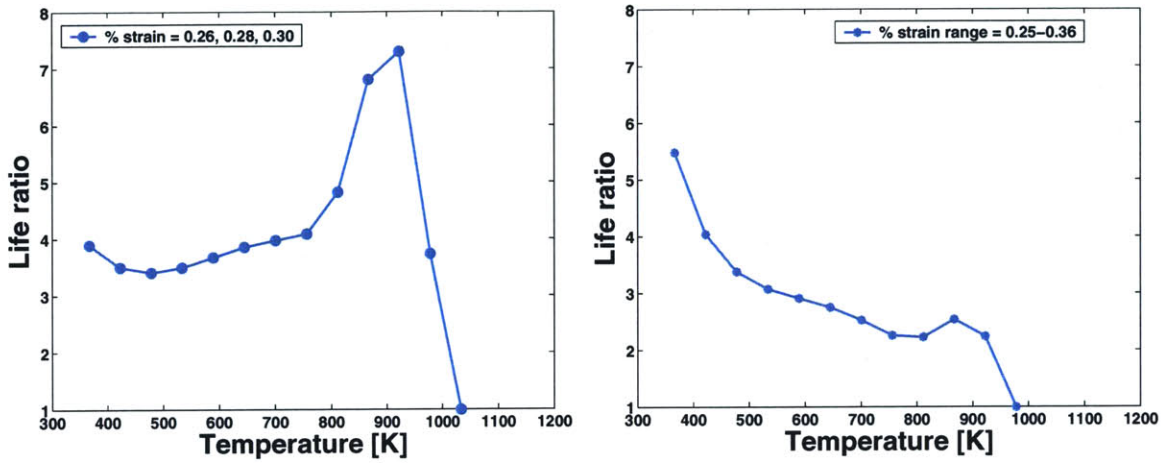

(a) (b)

Figure 2-2: Inconel 625 - changes in elastic life with temperature. (a) Elastic life estimates using constant strain values at different metal temperatures. (b) Elastic life estimates with temperature dependent strain

The most remarkable difference between the two figures is the overall behavior of the life ratio curve with decreasing temperature. In Figure 2-2a, the life benefit reaches a maximum around 900K and then decreases even with decreasing temperature. It appears counterintuitive that a greater life benefit is achieved at an intermediate temperature level; life benefits could be expected to continuously improve with decreasing temperature. This apparent contradiction is better understood if the stress levels associated with these strain values are examined. Figure 2-3 shows the stress levels corresponding to the imposed strains in Figure 2-2, normalized by the ultimate tensile strength of the material at the given temperature.

It is seen that in the constant strain case, the stress ratio is almost constant at lower temperatures and drops around the 900K temperature level by 0.02 or greater, resulting in the life ratio peak in Figure 2-2a. There is also a drop in stress ratio in the case of varying strain level as shown in Figure 2-3b, but this drop is only about 0.01 and more importantly, the stress levels increase with temperature. This drop in the stress ratio also results in a small peak in Figure 2-2b, but the overall trends are more reasonable than those of Figure 2-2a.

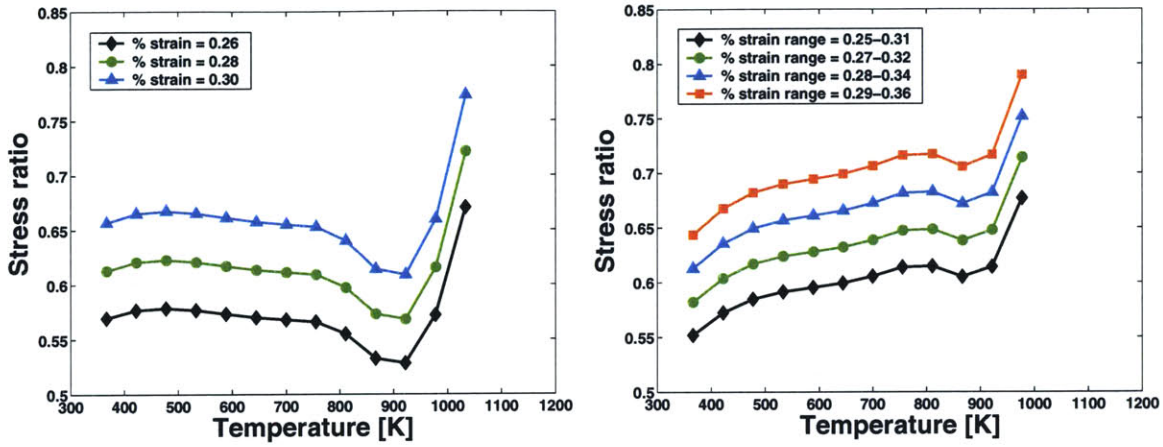

(a) (b)

Figure 2-3: Inconel 625 - ratio of imposed stress to ultimate tensile strength. (a) Stress ratio for the constant strain value case. (b) Stress ratio for temperature-dependent strain life estimates

Summarizing elastic behavior, it can be said that stress and strain levels that increase with temperature more accurately describe the physical process expected. For a blade metal temperature change between 34K to 47K, the elastic life improves anywhere between a factor of 2 to 3.2 depending on strain levels and temperatures for Inconel 625.

Similarly, the plastic life was also determined over the same strain ranges using equation (2.6b) for Inconel 625. The results are displayed below in Figure 2-4.

From equation (2.6b) it is seen that the plastic life is simply a function of ductility and strain values. Therefore, for constant strain, Figure 2-4a almost resembles the ductility curve for Inconel 625 (Figure 2-2a) and it is seen that there are no life benefits from decreasing temperature in the plastic life. However, in Figure 2-4b there is some life benefit seen only at very low temperatures.

The same analysis as above is repeated using the complete Universal Slopes method in equation (2.5), where the damped Newton-Rhapson method is used to solve equation (2.5) for N_f. The results are seen to strongly resemble the elastic life curves. Thus it is anticipated that the elastic life behavior will to a large extent determine the total life trends of the component.

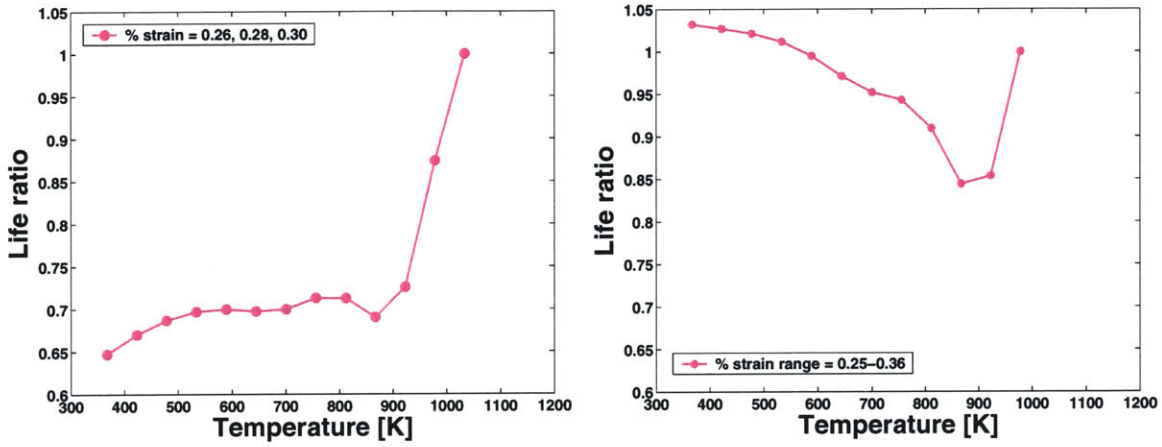

(a) (b)

Figure 2-4: Inconel 625 - changes in plastic life with temperature. (a) Plastic life estimates using constant strain values at different metal temperatures. (b) Plastic life estimates with temperature-dependent strain

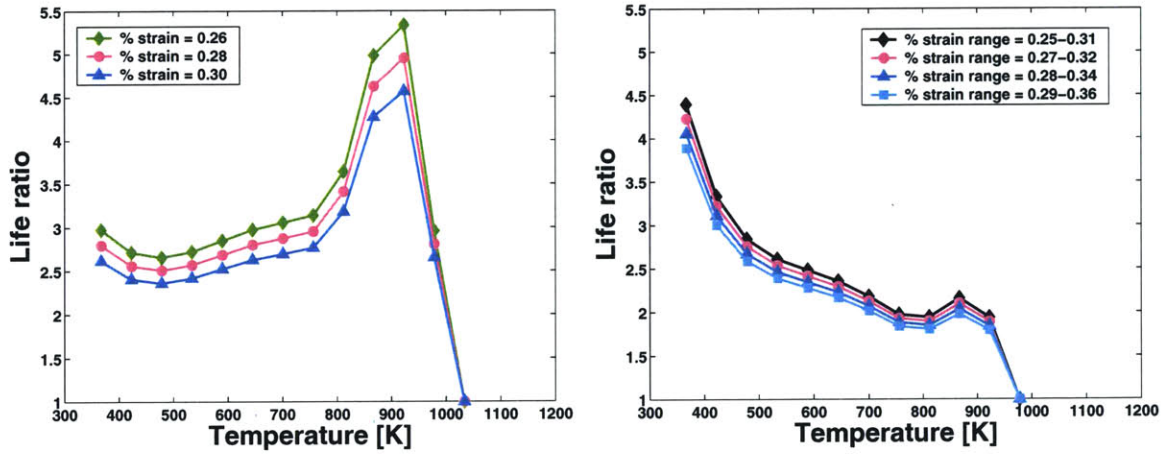

(a) (b)

Figure 2-5: Inconel 625 - changes in total life with temperature. (a) Total life estimates using constant strain values at different metal temperatures. (b) Total life estimates with temperature-dependent strain

Different strain ranges are investigated in Figure 2-5 and as anticipated, higher strain levels reduce fatigue life further. The curves follow the same general trends for varying strain levels and features from the elastic life curves are dominant. The plastic life part of the equation reduces the magnitudes of the life ratios as can be seen through comparing Figures 2-2 and 2-5.

The total life benefits now range from a factor of 1.9 to 2.5 for a temperature reduction of 67K in the turbine inlet temperature, depending on the stress levels and temperatures used for Inconel 625. This range includes results from both charts in Figure 2-5.

(ii) Inconel 706 and René 80:

Total life estimates with temperature dependent strain are shown for Inconel 706 and René 80 in Figures 2-6 and 2-7. The differences in life estimate trends of Inconel 706, Inconel 625 and René 80 primarily arise from variations in material properties.

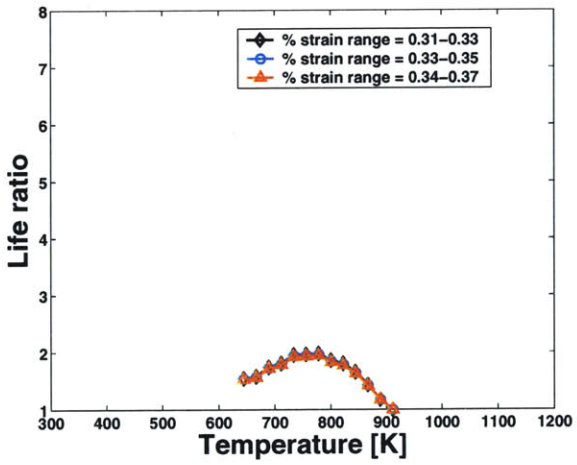

Figure 2-6: Inconel 706 total life estimates with temperature-dependent strain

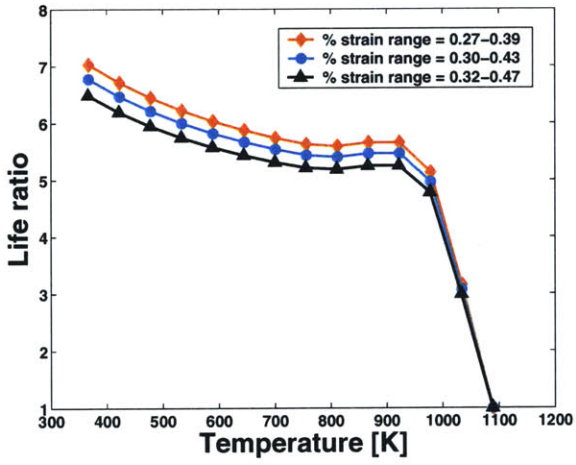

Figure 2-7: René 80 total life estimates with temperature-dependent strain

The range of temperatures used for Inconel 706 is narrower than that used for the other materials owing to data availability, and hence places some limitations on possible fatigue life trend comparisons. Despite the limitations, the general trend noted based on these three materials is that life benefits increase with decreasing

metal temperatures. With a 34K-47K reduction in turbine inlet temperature, life improvements range from 1.31-1.46 for Inconel 706 and by 2.39-2.85 for René 80 as seen from Figures 2-6 and 2-7. In contrast, from Figure 2-5b it is seen that fatigue life improves for Inconel 625 by 1.85-1.90 for the same turbine inlet temperature reduction and with strain levels that vary with temperature.

Thus, from these comparisons, given a known turbine inlet temperature reduction, a range of estimates can be provided for the expected improvement in turbine blade life. A more accurate estimate for life benefits can be obtained with a detailed analysis using the exact materials, blade geometry, coatings, temperatures and load levels involved in the specified engine type. Life benefits will also be dependent on the statistical validity of the basic data sets used in the analysis.

2.2.1.5 Effect of ambient conditions

There will also be differences in fatigue life benefits possible based on ambient operating conditions. At higher ambient temperatures, T_{t4} levels can be expected to be higher than at cooler ambient temperatures. As seen from Figures 2-5b, 2-6 and 2-7 the slope of the fatigue life ratio curve changes depending on the temperature range concerned; at higher temperatures the life curve slope is steep as compared to lower temperatures where the life curve flattens out. This indicates that for the same 34K-47K metal temperature reduction, it is possible for hot operators to encounter higher life benefits as compared to cold operators.

2.2.2 Creep and oxidation life estimates

Owing to the complex interactions between fatigue, creep and oxidation, a detailed life estimate analysis that accounts for component failure due to the combined effects of all the three mechanisms is beyond the scope of this study. In order to provide a preliminary estimate for life benefits from water injection, some relevant results found through a literature search are included in this chapter. Based on common industry practice [18], approximate changes in the first stage turbine blade life resulting from

changes in gas and metal temperatures as well as from centrifugal stresses are shown in Table 2.1.

Table 2.1: Turbine blade life estimates for creep and oxidation effects for varying temperatures and stresses [18]

Varying parameter	**1^{st} Stage Blade Creep-Fatigue life**	**1^{st} Stage Blade Oxidation life**
Local gas temperature ± 10K (mean 2000K)	± 15%	± 14%
Metal temperature ± 2.78K (mean 1000K)	± 8%	± 8%
Centrifugal stresses ± 1%	± 6%	—

Table 2.1 shows that large errors can result simply from errors in temperature or stress levels used for the analysis. It is very critical that the best estimates available for temperature and loads are used in life prediction methods to ensure reliable results.

The combined effects of thermo-mechanical fatigue and creep are usually studied experimentally and then modeled based on the data obtained. The tests include varying thermal and mechanical loads to simulate in-service working conditions. In a study by S.X. Li and D.J. Smith [19] the effects of temperature and cyclic loading were investigated on a single crystal nickel base superalloy, SRR99. The tests were carried out at 750°C (1023K) and 1050°C (1323K). The specimens were exposed to three different loading conditions, continuous cycling (denoted as 0/0), cycling with a tensile dwell, (t/0) and with a compressive dwell, (0/t). The tensile and compressive dwells were imposed to study crack initiation and propagation under combined fatigue and creep loading; the dwells were at constant strain for 2 minutes.

The results for crack initiation life and propagation rates are shown in Figures 2-8 and 2-9 and for both test temperatures; the triangles correspond to tensile strain dwells. Assuming tensile strains are more dominant in the case of turbine blades from centrifugal effects, from Figure 2-8 it can be noted that under tensile strain dwells, crack initiation life decreases as testing temperature increases. For approximately similar normalized strain levels, the crack initiation life changes from about

3000-5000 cycles for 750°C to around 200-400 cycles for 1050°C. Similarly, crack propagation rates increase with increasing temperature for tensile strain dwells as noted in Figure 2-9. For 750°C, propagation rates are about 0.0005 mm/cycle to 0.001mm/cycle; they increase by an order of magnitude ranging from 0.0025 to 0.004 mm/cycle at 1050°C. Additionally, it should be noted that the total strain range imposed at higher temperatures is less than that used at lower temperatures in order to observe the crack propagation behavior prior to complete failure. Thus, under tensile strain loads, the results of this study demonstrate that for alloy SRR99, crack initiation life decreases and crack propagation rates increase by an order of magnitude when the testing temperature is increased from 750°C(1023K) to 1050°C (1323K).

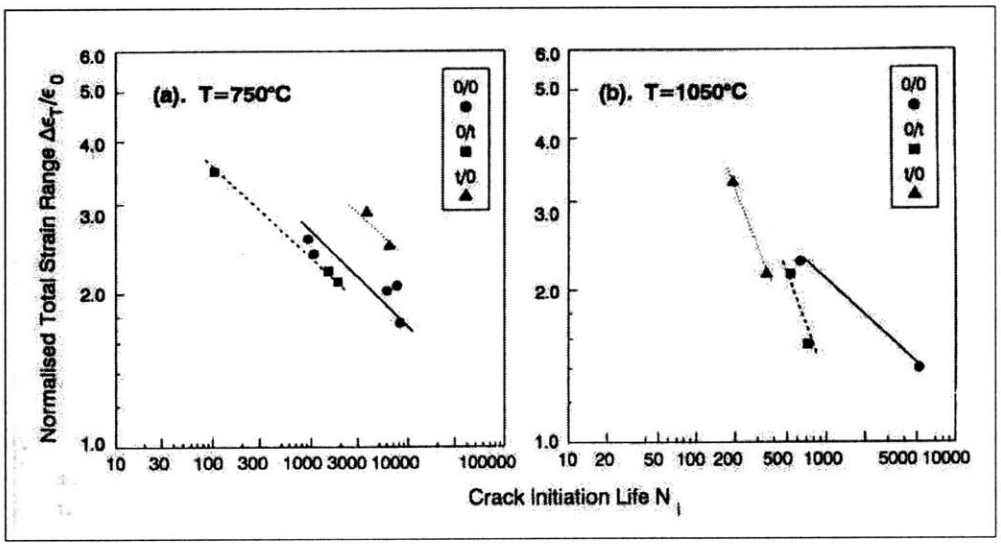

Figure 2-8: Influence of strain dwells and temperature on crack initiation life for SRR99[19]

Along with temperature and mechanical load effects, properties of the base alloys and coating materials involved are also deciding factors in the interactions between the different failure mechanisms. The protective coatings and the thermal barrier coatings (TBCs) impact the mechanical properties of the base alloy as well. The protective coatings are designed to shield the base material from environmental attacks while the TBCs reduce the effective temperature seen by the alloy. Due to the difference in material properties between the coatings and base materials, such as coefficients

of thermal expansion, tensile and compressive stresses are imposed on the coatings. Creep and cyclic loading result in cracking and spalling of the coatings exposing the alloys to higher temperatures and corrosive environments. Environmental effects need to be incorporated into the crack propagation models for the coatings and should be experimentally validated.

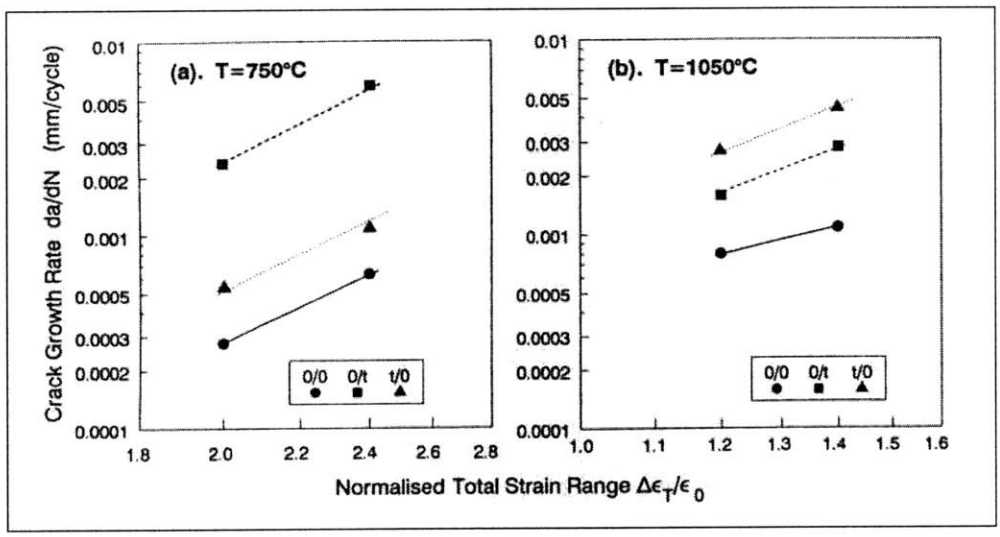

Figure 2-9: Influence of strain dwells and temperature on crack propagation for SRR99[19]

On a final note, estimates of potential turbine life benefits from water injection are also provided by engine manufacturers as a part of the Boeing study [6]. Pratt Whitney estimated life improvement by a factor of 1.29 and Rolls Royce predicted an improvement of upto a factor of 1.20 for a temperature reduction of 67K. Figure 2-10 compares the blade fatigue life estimates obtained from the Universal slopes method with industry estimates.

While the exact materials, methods and failure modes that correspond to these industry estimates are not known, they are comparable in magnitude to some of the estimates provided by the Universal Slopes method for fatigue life. Differences may be due to various factors including the detailed data used, life models and assumptions used, overall methodology etc. The exact range of possible life extension depends on the details of the parameters involved.

	Universal Slopes – Fatigue life Estimates			Industry Estimates[1]	
	Inconel 625	Inconel 706	Rene 80	P&W	RR
ΔT_{gas} (K)	-67	-67	-67	-67	-67
Life Improvement Factor	1.85 - 1.90	1.31 - 1.46	2.39 - 2.85	1.29 [2]	0 - 1.20[3]

Notes:

(1) **3k nmi mission length, 1:1 water to fuel injection ratio**

(2) **Turbine Service Life (1990's-2000 technology)**

(3) **Varies dependent upon engine operating conditions**

Figure 2-10: Summary of blade life estimates - Universal Slopes and industry estimates [6]

It is seen that the results of this analysis are strongly dependent on material properties, temperature and stress-strain ranges. The next section reflects on the shortcomings and key conclusions derived from the approach taken here to correlate turbine blade life to operating temperatures.

2.2.3 Summary and conclusions from the blade life analysis

The turbine blade life analysis presented herein is based on a generic approach to predict overall fatigue life trends using publicly available data for selected representative blade materials. The Universal Slopes method is used, which was developed from average values of material constants from experimental data available. In addition to the limitations imposed on the scope of the analysis due to the lack of detailed data, there are also some notable shortcomings in the application of the Universal Slopes method. The coefficients used in equation (2.5) are obtained through isothermal, room temperature fatigue tests done on a wide range of materials. As shown in the Manson report [14], these average coefficients provide fairly reliable life estimates for the 29 materials tested with 99.5% of the experimental data falling within a factor of 20 of the predicted life. However, life estimates obtained under thermo-mechanical fatigue (TMF) can vary significantly from those obtained from isothermal low cycle fatigue. Under in-service conditions, turbine blades are exposed to widely

varying thermo-mechanical loads and simplified isothermal models do not capture the complexity of the situation. The deviation of isothermal results from TMF results depends largely on the material properties and the nature of the TMF cycle. The primary reason for the use of the Universal Slopes method in this analysis was the ease involved in its use and availability of the necessary material data. Regardless of the limitations involved, this method is an appropriate tool for a preliminary design level analysis where the overall trends in life behavior are sought. For instance, the Universal Slopes method has also been used as a part of the fatigue life analysis in the Space Shuttle Main Engine (SSME) design process, to obtain life estimates where no or limited fatigue data were available [20].

In order to enhance the accuracy of the Universal Slopes method, these material constants would have to be determined experimentally for the blade material in question. Other methods that predict life more accurately can also be used if more data are available that account for the interactions between the different failure mechanisms, namely creep, oxidation and fatigue. Effects of creep can be incorporated into the crack propagation analysis mentioned previously. It is difficult to capture the effects of oxidation in a generic study like this since details about the nature of the protective coatings and their impacts on the base alloy are complex phenomena and are proprietary. Despite the shortcomings of the methods applied in this study, it can be said with confidence that improvement in turbine blade life is expected with decreased turbine inlet temperature.

2.3 Material maintenance cost estimation

To assess the impacts of water injection on turbine durability, it is necessary not only to quantify turbine blade life impacts, but also to address the potential maintenance costs benefits. Turbine inlet temperature reduction from water injection can be compared with similar reductions achieved from engine de-rated takeoff operations. Airline data [21] available for material maintenance costs associated with de-rated operations for a 1970's technology mixed flow turbofan engine are used to estimate

the cost benefits associated with water injection. Engine cycle-deck results from GasTurb [10] are utilized in correlating the 67K change in T_{t4} to takeoff de-rate levels. The maintenance cost analysis is then presented in the form of percent reductions in cost for the de-rate levels and for different flight times. It is important to note that while the results for the turbine life blade analysis are generic, the maintenance cost analysis is done for a specific engine based on data availability and is therefore only an example of potential cost benefits.

2.3.1 Takeoff thrust de-rate

It is common practice to operate at de-rated thrust levels at takeoff as well as during climb in order to achieve lower operating temperatures. This usually increases takeoff time, however, the engine maintenance cost benefits generally outweigh the disadvantages associated with an increased fuel burn. According to a major airline, de-rated takeoffs are performed for 67%-95% of flights depending on factors such as aircraft type and weight, weather conditions and runway length, with typical de-rate levels ranging from 5% to 25% [21]. While the time spent at peak temperature levels during takeoff is a small fraction of the total flight time, it is a crucial factor for engine maintenance costs. The takeoff segment constitutes about 1% of the total mission time and yet is responsible for 60% of total engine wear [22]. Figure 3-1 shows the flight time and engine maintenance cost distribution between the different mission segments.

Peak temperature levels during the takeoff segment are a significant driver of hot section overhaul costs as noted in Figure 3-1. Lowered temperatures in the engine hot section resulting from de-rated operations lead to extended engine life. Data obtained from an airline show maintenance material cost reductions due to de-rated operations [11]. These data only reflect basic causes for maintenance including Foreign Object Damage (FOD), but do not include negligence or labor costs.

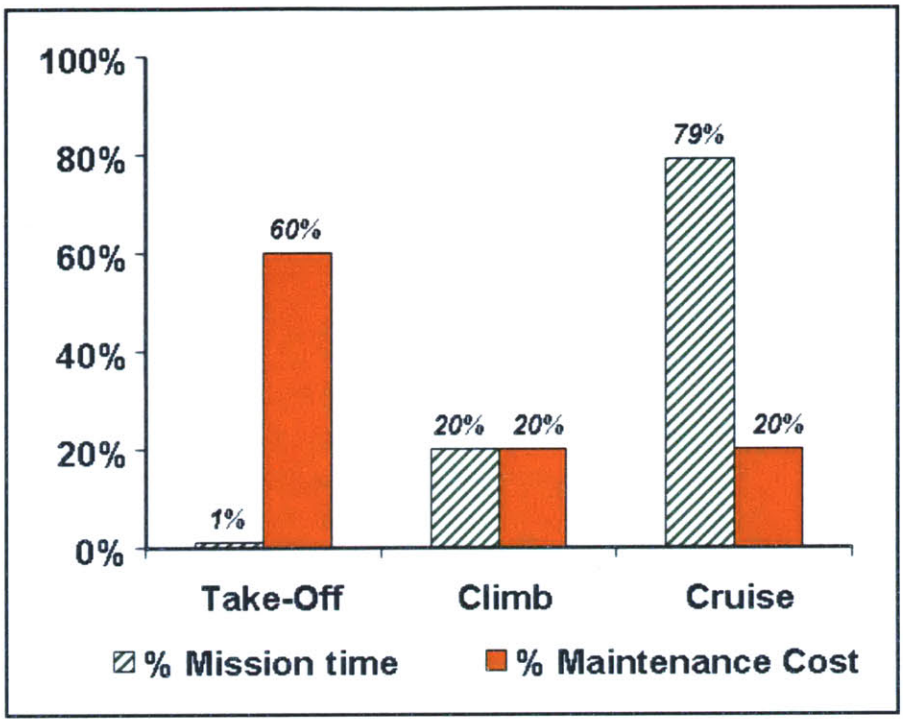

Figure 2-11: Mission time segments and associated engine maintenance cost impacts[22]

De-rate levels can be correlated with reductions in turbine inlet temperature to establish a relationship between cost reductions and turbine inlet temperature. Since water injection also results in lowered turbine inlet temperatures, potential maintenance cost benefits are likely. The airline maintenance cost data is used to estimate cost benefits possible due to water injection.

In order to connect de-rate levels to changes in turbine inlet temperature, cycle deck analyses are performed in GasTurb [10] to observe the influence of several cycle parameters on the off-design relationship between thrust and T_{t4}. Different engines cycles are analyzed through GasTurb [10] by varying OPR, BPR, T_{t4}, component polytropic efficiencies and the mass flow. Linear trendlines are fitted through the cycle deck data obtained. The slope of the trendline for each cycle is the ratio of change in the net thrust to change in T_{t4} and has the units of [kN/K]. The average, minimum and maximum values of this slope are determined from the cycle data and used to relate the 67K change in T_{t4} to a corresponding change in thrust. The details

of this cycle analysis are shown in Appendix A. For a reduction of 67K in T_{t4} from water injection, the change in thrust is found by:

$$\Delta\text{Thrust (de-rate)} = 67\text{K*slope} \tag{2.8}$$

The percent de-rate is calculated simply by dividing the Δ Thrust values by the takeoff thrust for each cycle and then averaging the results. This percent de-rate is assumed to be the takeoff de-rate and is then combined with the airline data to obtain maintenance cost reductions due to water injection. It is important to note that there maybe differences involved in blade heat transfer mechanisms in the de-rate process as compared to water injection. In de-rated operations, there is a reduction in T_{t4} as well as in the blade cooling flow temperature. However, for water injection in the combustor, only T_{t4} is lowered while the cooling flow is unaltered. Hence, the change in blade temperature may not be the same for two procedures leading to different maintenance cost improvements. However, for simplifying the analysis, it is assumed here that the same maintenance cost benefits are possible for water injection and takeoff de-rate. A more accurate answer can be obtained if a heat transfer analysis is done to obtain the ΔT_{t4} needed from water injection as compared to the ΔT_{t4} in the de-rate procedure, to match the blade metal temperature change resulting from the de-rate procedure.

2.3.2 Material maintenance cost benefits

The maintenance cost estimates for water injection are extracted from the available airline data, by correlating T_{t4} reductions from de-rated operations to changes in T_{t4} resulting from water injection. Based on this first order analysis it is seen that the throttle curves are not very sensitive to changes in most of the key engine cycle parameters. Table 2.2 shows the average, maximum and minimum values of the slope of the linear fits to the cycle deck data. From equation (2.8) it is seen that these slopes relate the ratios of change in the net thrust to change in T_{t4} with units of [kN/K]. Also indicated in Table 2.2 are the % de-rate values corresponding to the

average, minimum and maximum values of the slope for a change in T_{t4} of 67K from water injection.

Table 2.2: Average, minimum and maximum values of the thrust de-rate from water injection

	Slope [kN/K]	% De-rate
Minimum	0.13	5.1
Average	0.21	8.4
Maximum	0.29	11.5

It is seen that depending on the engine cycle data used, the % de-rate value corresponding to water injection can range from 5.1% to 11.5%. The cost benefits resulting from the equivalent water injection thrust de-rate are calculated based on the airline maintenance material cost data mentioned previously. Only the effects of takeoff de-rate caused by water injection are evaluated in this analysis. Table 2.3 shows the percent reduction in material maintenance costs per engine flight hour (MMC/EFH) in 2004 dollars for three different flight lengths as well as for the different takeoff de-rate values. The baseline from which these reductions are calculated is the material maintenance cost with no de-rate for each different flight length. Overall, it is seen that costs decrease with increasing flight time which is expected since longer flight times indicate that a small portion of the flight is spent at critical takeoff level temperatures. Costs also decrease with increasing de-rate levels, since this reduces the effective operating temperature.

Table 2.3: % reduction in MMC/EFH in 2004 dollars for a range of takeoff de-rates and flight lengths

Takeoff de-rate (%)	1 hour (%) change	6 hours (%) change	12 hours (%) change
5	10.43	6.06	1.90
8.4	16.52	9.09	2.86
11.5	20.87	10.61	3.81

Thus, it can be seen that maintenance material cost benefits are possible from a T_{t4} reduction of 67K from water injection. The benefits possible depend on the flight length and values of de-rate corresponding to the T_{t4} reduction obtained from the engine cycle deck. It is important to remember again, that this analysis only represents a single engine. However, the results are significant in that for this engine a narrow range of possible reductions in cost can be presented with confidence. This method of assessing costs relies primarily on data available from industry. A greater level of confidence can be placed in the results if the engine in question can be simulated in a more advanced cycle deck than GasTurb [10]. Since the throttle curves did not show much variation with changes in cycle parameters, this study provides a good preliminary estimate of cost benefits from water injection.

2.4 EDS engine durability and maintenance cost estimation capabilities

The Environmental Design Space is a numerical simulation tool for estimating aircraft noise, emissions, performance and cost parameters. It fits in the larger APMT framework described earlier in Chapter 1 and provides the capability of assessing different technology scenarios. Quantifying the impacts of introducing new low emissions technologies on aircraft performance and costs is critical to gauging their implementation feasibility. Water injection, discussed in this chapter, is one such technology that holds the potential for NO_x reductions by lowering operating temperatures in the engine hot section. It has already been seen through the previous discussion that water injection may lead to savings in turbine life depending on the turbine materials, loads and temperatures. This section presents an inquiry into the capability of EDS to provide component life predictions and maintenance cost benefits. Using water injection as an sample technology the key question asked is: Does EDS version 1 currently have the capacity to conduct the type of analysis shown here and if not, can it be modified to do so?

EDS version 1 does not have the capability to predict any engine component life. Based on the results of this chapter, it is known that a generic physics-based model or approach does not exist for capturing the effects of all the principal failure modes in the engine hot section. Component life prediction is strongly dependent on material selection, detailed part geometry and accurate estimation of operating conditions - loads and temperatures. While some of these data can be approximated through the Weight Analysis of Turbine Engines (WATE) program in EDS, it is primarily the lack of reliable generic life prediction models that poses an obstacle to developing a durability estimation capability in EDS. Only empirical models such as the Universal Slopes Method are currently available for generic component life prediction. Such methods are adequate for predicting part life trends or overall behavior, but may have large uncertainties in the absolute values of the results obtained. Other shortcomings of the Universal Slopes Method have been discussed previously in Section 2.1.3 and will not be repeated here. Also, the Universal Slopes Method only accounts for low cycle fatigue in the turbine components. Creep, oxidation and other corrosive effects are not captured in generic models. As mentioned earlier, experimental data is usually needed to develop models for creep and oxidation failure modes and such models tend to be specific to the material in consideration. Owing to these considerations, it is unlikely that EDS will be able to develop and incorporate a detailed physics-based engine durability modeling capability.

The Aircraft Life-Cycle Cost Analysis Code (ALCCA) module in EDS is responsible for assessing maintenance costs. Maintenance cost estimation done in ALCCA is based on empirical methods and includes factors such as mean time to repair, engine removal rates, average time between overhauls, labor and material costs and operating temperatures [23]. This relates to the approach used in this chapter to estimate maintenance cost benefits from water injection. Potential maintenance cost benefits from water injection were quantified by correlating temperature reductions due to water injection to those from de-rated operations. Airline data on material maintenance cost benefits from takeoff thrust de-rate were used to estimate maintenance cost benefits from water injection. While this approach was more restrictive, since

the trends obtained were applicable to a specific engine, it was based on airline data - giving it better credibility than the Universal Slopes approach.

The same deduction applies to ALCCA capabilities - where maintenance cost estimation based on historical data and empirical economic methods can be considered to be more reliable than part life prediction based on empirical models. The physics and chemistry involved in the hot section of the turbine are too complex to be completely captured by a generic empirical model. An economics-based approach using historical trends in operating costs and the breakdown of different components of maintenance costs may be a more reliable option in this case. This hypothesis is supported by the observations based on the results of this chapter. A rigorous analysis of the cost prediction methodologies in ALCCA is necessary to validate this hypothesis. This line of reasoning can also be extended to the general EDS framework. For the analysis presented in this chapter, a physics-based approach was used in the Boeing water injection study [6] to determine reduction in T_{t4} possible from injecting water in the engine combustor. However, due to the complexity of the phenomena associated with the failure mechanisms and lack of data due to its proprietary nature, it was necessary to use empirical methods to obtain life estimates. This approach of complementing physics-based approaches with empiricism is also applicable and important throughout the EDS module.

Chapter 3

Cruise Speed-BPR Trade Study and Operator Cost Sensitivities

Airplane design is primarily dictated by tradeoffs between increasing fuel efficiency and reducing environmental impacts while keeping the product economically viable for the customers-the airlines. Increased fuel efficiency typically translates to a decline in environmental impacts due to the lowering of emissions. Ideally, it is desirable to achieve both effects, of reducing fuel usage while also increasing profit margins. It is important to note the difference between an airplane that is very fuel efficient but is not necessarily more profitable as compared to one that needs more fuel for a given mission. For instance, the improved fuel efficiency may come with the use of advanced technologies that increase maintenance costs or have other such cost related impacts, such as increased weight. However, with ever-increasing fuel prices, fuel efficiency may become a more critical design driver for future airplanes. Technological advances as well as operational strategies can help in improving the fuel efficiency of airplanes and in effectively reducing emissions.

This study looks at the impacts of implementing advanced technology engines with ultra-high bypass ratios and of varying cruise speed on the fuel efficiency of future airplane designs. Both these strategies have the potential to reduce aircraft fuel burn. Fuel burn may become an even more critical design driver in the future either due to escalating fuel prices or from the introduction of environmental costs

such as emissions taxes or trading. These additional costs may be in the form of artificial costs imposed on fuel prices. The tradeoffs presented in this study propose potential strategies to offset rising fuel costs and possible environmental costs using technological and operational changes.

Inputs used in this analysis consist of proprietary data obtained from Boeing Commercial Airplanes and the performance analyses were done using Boeing internal tools. For the purpose of this analysis, a baseline 737-sized study airplane with advanced technology engines was selected. The study engines selected included a set of high bypass ratio engines from the NASA Ultra Efficient Engine Technology (UEET) initiative [24] and a second set of proprietary geared fan engines. The effects of engine BPR and cruise speed on mission fuel burn were examined for a fixed economic range of 500 nautical miles.

Additionally, results obtained from this performance analysis were used in a sensitivity study on operating costs, with BPR, cruise speed and fuel price as the key variants. Changes in Cash Airplane Related Operating Costs (CAROC) were calculated using data from a comparable, small, single-aisle transport as the baseline to assess the implementation feasibility of these advanced technology engines and of varying cruise speed under different future fuel price scenarios.

This chapter initially presents a brief discussion of the inherent complexities involved in the BPR and cruise speed trade study in relation to operating costs and other considerations. Next, the assumptions and methods used and results from the BPR, cruise speed and CAROC analysis are described. In the concluding remarks, the shortcomings of this study along with areas of future work are identified.

3.1 Key considerations for the BPR and cruise speed trade studies

Prior to discussing the details of the analysis for both studies, the following questions are briefly addressed: what can be hoped to be achieved by incorporating these

changes in airplane design? What results are expected? The selection of the figure of merit is very important in the determining the final airplane design. Such questions are addressed separately for both studies in this section.

3.1.1 BPR trade study

The NASA UEET report [24] mentioned previously, includes an engine diameter trade study for a 305-passenger future study airplane using the advanced technology, ultra-high BPR, UEET engines. The bypass ratio range for these engines is from 11 to 22. All three engines have a thrust level of 78,800 lb at Mach 0.25. Based on the results of this report, increasing BPR improves SFC performance; however, the upper limit on the optimal engine fan diameter is placed by drag and weight considerations. As engine fan diameter increases with engine BPR, weight and drag penalties offset the SFC benefits from the larger engines. Figure 3-1 shows relevant SFC and mission block fuel characteristics for these engines.

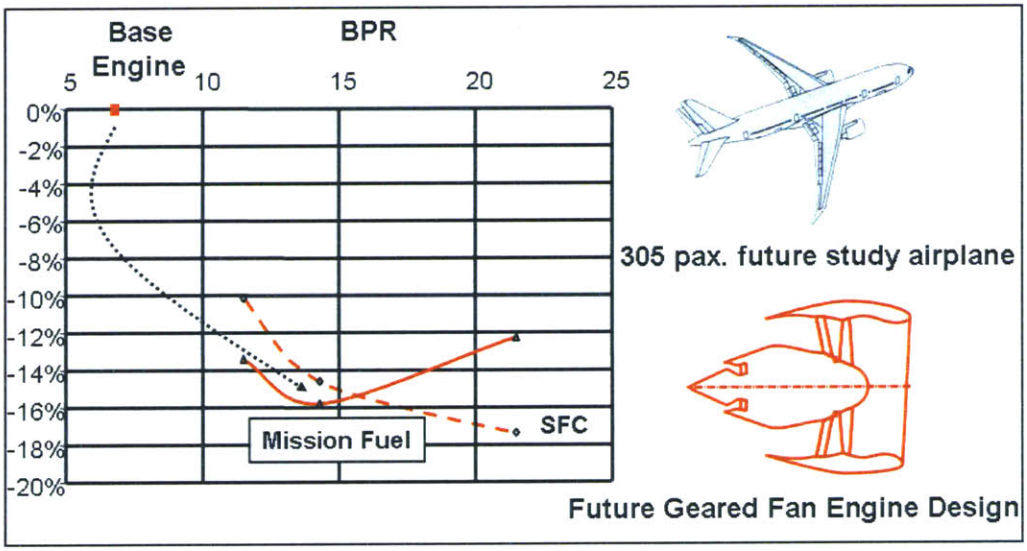

Figure 3-1: UEET engines SFC and block fuel savings [24]

The improvement in SFC with increasing bypass ratio is indicative only of the engine performance, ranging from 10% to about 18%. The block fuel savings are calculated based on an installed performance analysis, accounting for combined effects of airframe weight changes and improved engine performance. While engine SFC

savings increase with BPR, block fuel savings are affected not only by SFC changes and weight changes, but also by drag penalties due to increasing engine diameter at high bypass ratios. Figure 3-1 indicates an optimum bypass ratio of about 14 with a 16% reduction in mission block fuel with the installed performance.

The results in Figure 3-1 are all obtained for a cruise speed of Mach 0.85. The results of the UEET study are also extrapolated to smaller and larger airframes. For smaller airframes, BPR increases also influence factors such as engine ground clearance, gear length and vertical tail area. Larger engines increase windmilling drag during engine out conditions. To compensate the yawing motion of the airplane, a larger rudder size and vertical tail area is necessary. A BPR of about 14 was also found to be optimal for both the smaller airplane and the larger airplane[24].

This chapter attempts to identify the optimal bypass ratio configuration for a smaller 737-sized airframe, but also at lower design cruise speeds. The UEET engines are used for this study and have been scaled down for smaller airframe requirements. No noise reduction possibilities or changes in nacelle design are addressed. The main focus of this analysis is evaluate how BPR changes translate to fuel savings and if this leads to any reductions in operating costs for a 737-sized airplane. In other words, fuel efficiency as well as economic viability are examined for varying BPR on a small airframe. This is only a first attempt at the problem, made with simplifying assumptions to initiate an inquiry; the shortcomings of these assumptions and areas that need an in-depth analysis are highlighted later in the chapter. The next section discusses the complexities involved in conducting a cruise speed study.

3.1.2 Cruise speed study

Based on first principles, it is reasonable to expect fuel savings upon reducing cruise speed. This premise needs to be explored further to understand the tradeoffs involved in flying slower and thus for a longer duration and gauge what benefits are possible by doing so. The author spent some time talking to several people in the Boeing Company specializing in preliminary design - aerodynamics as well as configuration, to address this question.

The problem of assessing what is the right cruise speed is a multi-layered and multi-faceted one. It also depends on what the objective is - that is the variable that is being optimized. An analysis to simply minimize block fuel may not give the right solution for minimizing operating costs. Operating costs are driven by several factors such as fuel costs, landing fees, servicing fees, and time related costs such as crew salaries and maintenance costs. A discussion on the tradeoff between time and fuel related costs is presented in Carlos E. Padilla's book [25]. He presents an approach where the distance traveled per unit cost is maximized by incorporating fuel and time costs. Maximum range is obtained for two different cases, one that only considers fuel burn and a second one that also includes time related costs along with fuel costs. The optimum cruise speed for the maximum range that considers only fuel burn is lower than that which also accounts for time costs. This is also seen in Nicolas Antoine's Ph.D. thesis [26], that looks at multi-objective trade studies with two of the objectives being low cost and low fuel. The minimum cost design flies at a higher cruise Mach than the minimum fuel airplane. The question then is: when does fuel cost become a more important driving factor for operating costs? In summary, this study tries to analyze how cruise speed should be varied to reduce fuel costs under different fuel price scenarios. Fuel cost escalation maybe due to direct increases in jet fuel prices or based on emissions related charges artificially imposed on fuel prices. Thus, this study also demonstrates how cruising slower maybe a potential strategy for reducing fuel usage and consequently reducing environmental impacts and costs.

Another important consideration is how the problem is defined in terms of assumptions made, constraints set and which mission is examined. As an initial attempt at this problem, several simplifying assumptions are made and performance constraints are set to clearly define the problem and obtain some results. This is treated as the starting point of the analysis and is by no means "the right answer". The purpose of this study is to examine trends in fuel usage and in operating costs if cruise speed were to be varied. The author acknowledges that depending on which performance constraints are set as rigid or flexible, the solution obtained may show a different design. Only the direct operating costs for a single airplane trip are considered. Pas-

senger related indirect costs such as food and other such services are not accounted for. Change in flight speed may result in appropriate changes in such services; for instance, more food may need to be carried on board if the flight time is significantly increased. Additionally, productivity costs are not addressed here; productivity costs refer to the utilization of the airplane for generating maximum revenues by the airlines. A fleet level analysis is necessary to understand the impacts of cruise speed on the overall operating economics of the airlines. Such detailed economic analyses are beyond the scope of this study and are indicated as areas of future work. Other global considerations such as operational constraints imposed by the ATC and their impacts on slower cruising airplanes are also not explored here.

Finally, the results are based on an economic analysis mission range of 500 nautical miles with a design range of 3000 nautical miles. While the airplane is sized for the design range of 3000 nmi, the performance for the 500 nm range is examined to understand the effects of varying cruise speed. This may result in an airplane that is configured best to fly the economic range, and while it is capable of covering the design range, it may not be economically advisable to fly the design range at the determined cruise speed. In other words, while cruising slower may be beneficial for the shorter range where time effects are not felt as much, it may not be the optimum solution for the design range. Cruising slower may be an option only for short missions. Since cruise Mach number is an important design parameter that strongly dictates airplane configuration, the configuration requirements for the economic range could be different from those for the longer design range. The best configuration should be selected based on customer mission requirements. In order to begin addressing all these questions, it is necessary to do a first order analysis investigating the effects of cruise speed.

3.2 BPR and cruise speed: assumptions and study results

As mentioned previously, two different sets of engine performance models (i.e. decks) were used for this study. The NASA UEET engines were used initially and the study was repeated upon the availability of an updated set of advanced technology engines. The new engine set was used since it was understood to be more suitable to the study in terms of size and characteristics for a 737-sized airplane. Detailed information about engine characteristics cannot be presented here due to the proprietary nature of the data. Repeating the analysis using the new set of engines also provided an opportunity to validate the trends observed from the results of the previous UEET analysis. Additionally, for the UEET engines, Mach 0.65, 0.75 and 0.85 were used for the cruise speed study. For the advanced technology engines, cruise Mach 0.6, 0.7 and 0.8 were used.

3.2.1 Key assumptions

The baseline airplane was sized for a total of seven different engines, three from the UEET set and the remaining four from the updated data set. Boeing tools for mission analysis and optimization were used for the climb, cruise, descent and reserves flight segments. A baseline airplane configuration was input along with engine data tabulated for different mission segments. The baseline engine data was supplied by engine manufacturers, while some off-design point data was supplied by Boeing. Based on the constraints and objective functions specified, the tools run a mission analysis and output the optimum route/mission. Mission block fuel and block time values were obtained for each run. The assumptions used and the performance analyses done for both sets of engine decks were identical. The main assumptions in the analysis are:

(i) BPR study:

1. The baseline airplane was sized for the different engines for a fixed design range of 3000 nmi by varying the wing area and the thrust required at Mach 0.25 during takeoff.

2. Takeoff field length(TOFL) and approach speed (V_{app}) were used as performance constraints in the sizing process such that the resized airplanes would match the performance of the baseline airplane. Wing area sizing is driven by approach speed limits, while takeoff field length depends on the engine thrust level.

3. The economic mission range was 500 nmi.

4. For the UEET engines, baseline cruise Mach was 0.85.

5. For the advanced technology engine set, baseline cruise Mach was 0.80.

6. With each engine used, thrust and fuel flow tables were input along with changes to airplane operating empty weight (OEW) and to nacelle drag based on engine diameter correlations.

7. Based on the takeoff thrust requirements from the sizing process, the engine air mass flow through the fan was changed by scaling the engine diameters to extract the necessary thrust.

(ii) Cruise speed study:

1. The basic assumption was that the same $(M\frac{L}{D})$ [1] performance could be extracted by the wing flying at different cruise Mach (the physical details of wing design were not considered).

[1]Specific range for a jet-powered airplane is defined as: $\frac{mi}{lb} = M\frac{L}{D}\frac{a}{(SFC*W)}$
$M\frac{L}{D}$ is a measure of the aerodynamic efficiency of the airplane for the specific range capability
a=the speed of sound [mi/hr], W=the airplane gross weight [lbf], SFC=the engine specific fuel consumption[(lb/hr)/lbf]

2. Airplane drag rise characteristics were held constant at the baseline values by by shifting the baseline drag polars by:

   $\Delta M = M_{cruise} - M_{baseline}$

3. Buffet altitude was assumed to not be limiting at any Mach number.

4. C_L and C_D were multiplied by appropriate factors to hold optimum flying altitude the same and to keep $M\frac{L}{D}$ the same even for different cruise Mach numbers.

5. Specific fuel consumption (SFC) and weight changes to try and optimize the engines for flying at different cruise M were included for the UEET engines. This information was not available for the updated advanced technology engines and hence those engines were not modified for flying at different cruise speeds. For the updated engine set, the speed study was done by only adjusting the drag polar as mentioned previously. This may affect engine SFC performance and weight approximations since the advanced technology engines were not re-optimized for flying slower.

3.2.2 BPR-cruise speed study results

Results from the performance analysis showing trends in mission block fuel use for varying bypass ratio and cruise speed are presented. For a fixed economic range of 500 nautical miles, the baseline airplane is sized for the different engines and the performance is evaluated for varying cruise speeds. The metric used to assess performance impacts is the mission block fuel per seat. Figures 3-2 and 3-3 show the results of this study for the UEET engines and the updated engine set respectively.

From Figures 3-2 and 3-3, it can be seen that at the highest cruise Mach number there is a clear optimum BPR value that minimizes block fuel per seat. For the UEET engines at cruise Mach number 0.85, the optimum BPR is approximately 14. However, as the cruise speed is lowered for both engine sets, block fuel per seat decreases with increasing bypass ratio. The results of the performance analysis show that while flying at low cruise speeds, greater savings in mission block fuel use are encountered as BPR

increases. According to these results, the drag and weight penalties associated with higher BPR engines are less critical as cruise speed is lowered. M 0.65 results in Figure 3-2 and M 0.60 in Figure 3-3 show that there are block fuel savings even with the biggest engines and the minimum of the block fuel bucket might occur at higher bypass ratios.

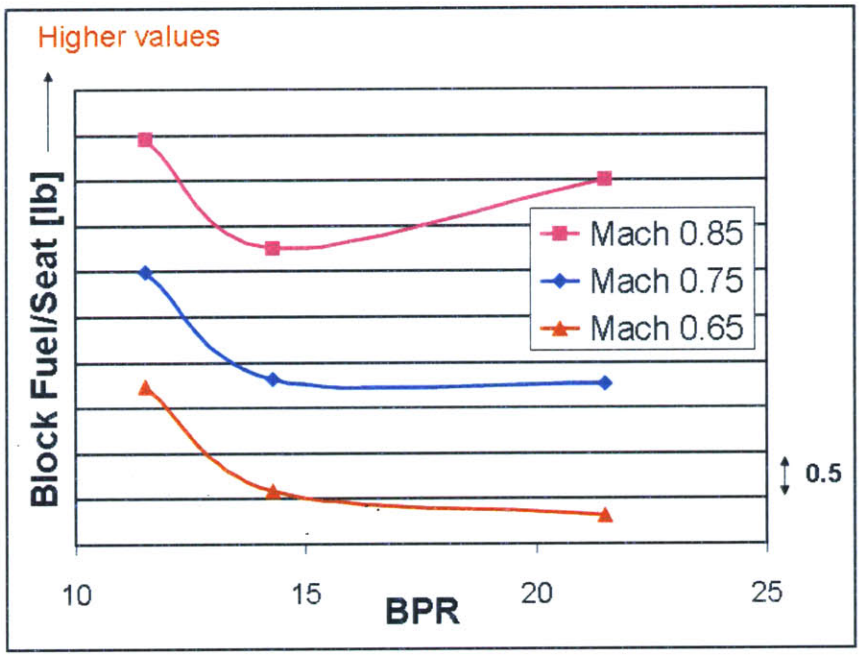

Figure 3-2: UEET engines block fuel per seat trends for varying bypass ratio and cruise speed

Overall, UEET engine results show greater sensitivity to changes in BPR as compared to the updated, advanced technology engines. However, it is important to note that there is a difference in the BPR axes of the two figures; while Figure 3-2 shows a total change in BPR of 11 units from the highest to the lowest value, in Figure 3-3, BPR only varies by 4 units. This difference exaggerates the perceived sensitivity of block fuel per seat to BPR for the UEET engines. The next part of the study assesses impacts of varying BPR and cruise speed on CAROC.

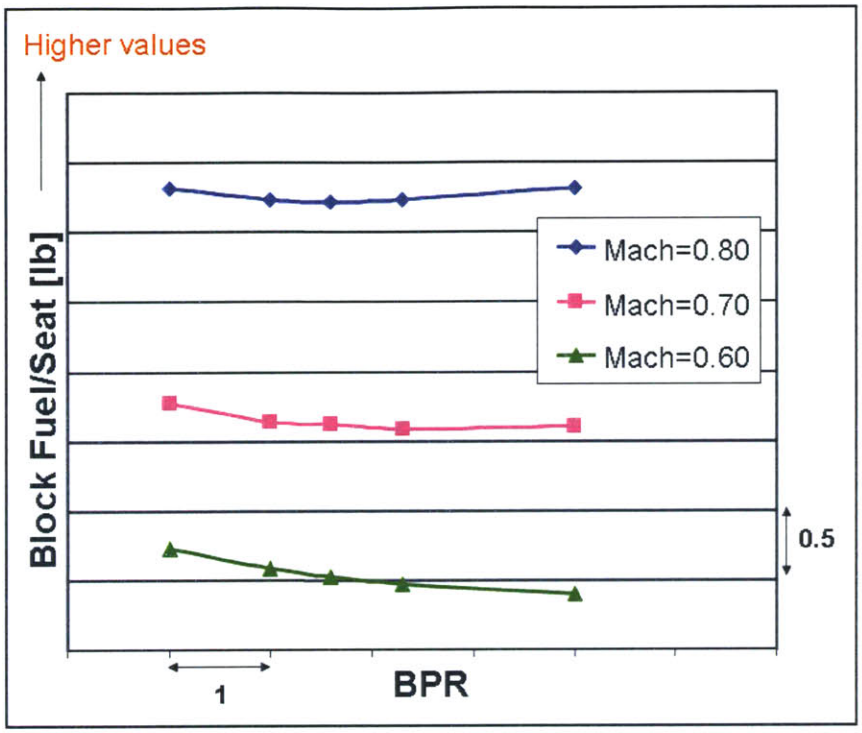

Figure 3-3: Proprietary engines block fuel per seat trends for varying bypass ratio and cruise speed

3.3 CAROC analysis and assumptions

The CAROC analysis was done using the mission block fuel and block time values obtained from the performance analysis described previously. Changes in CAROC relative to the baseline values were calculated based on the corresponding differences in block fuel and block time values. Different fuel prices were used to assess the impact of fuel price scenarios on CAROC sensitivity to bypass ratio and cruise speed. The main assumptions in this analysis were:

1. Baseline CAROC data from a comparable, small, single-aisle transport airplane was used in this analysis.

2. Only three components of CAROC - cabin and flight crew, fuel and maintenance costs were variables, all the other components were assumed to be the same as the baseline values.

3. Crew and maintenance costs were functions of mission block time.

4. Fuel costs were a function of mission block fuel use and fuel price.

5. Two different fuel price scenarios were evaluated - about $1.50 per gallon, and between $1.50 per gallon and $3.00 per gallon.

6. Costs for the baseline airplane were calculated for the same fuel price scenarios used on the study airplane for CAROC comparisons.

7. Utilization costs resulting from possible changes in the number of flights per day were not accounted for.

3.3.1 CAROC study results

Trends in operating costs with varying cruise speed and fuel prices are shown in Figures 3-4 and 3-5. Each figure shows the results for a specific engine and hence for a fixed bypass ratio. Figure 3-4 shows the data for an engine from the UEET set while Figure 3-5 gives the trends for an engine in the second, updated set.The percent changes in CAROC and block fuel in Figures 3-4 and 3-5 are with respect to the baseline airplane. For both sets of engines, costs savings are encountered in comparison to the baseline. Mission block fuel and block time are the driving factors in quantifying the savings possible from using these advanced technology engines and in cruising slower. Flying slower leads to reductions in block fuel use, but increases mission time, therefore increasing crew and maintenance costs. The general trend observed is that greater savings can be obtained by flying faster when fuel prices are low. This is because block time related expenses such as crew and maintenance costs are more critical than block fuel costs.

However, it is significant to note the effect of increasing fuel price. Here the baseline costs are also calculated using the same fuel prices for a fair comparison. In Figures 3-4 and 3-5, as fuel price is increased, operator cost savings become less sensitive to cruise speed. The study airplane with new technology engines offers better savings in operating costs at higher fuel prices. CAROC benefits are also to be noted at reduced cruise speeds. The cost optimal point at a fuel price of about $1.50 per gallon is at a cruise speed of Mach 0.85. As fuel price is increased to about $3.00 per gallon, the cost optimal point shifts to a cruise Mach number of 0.75.

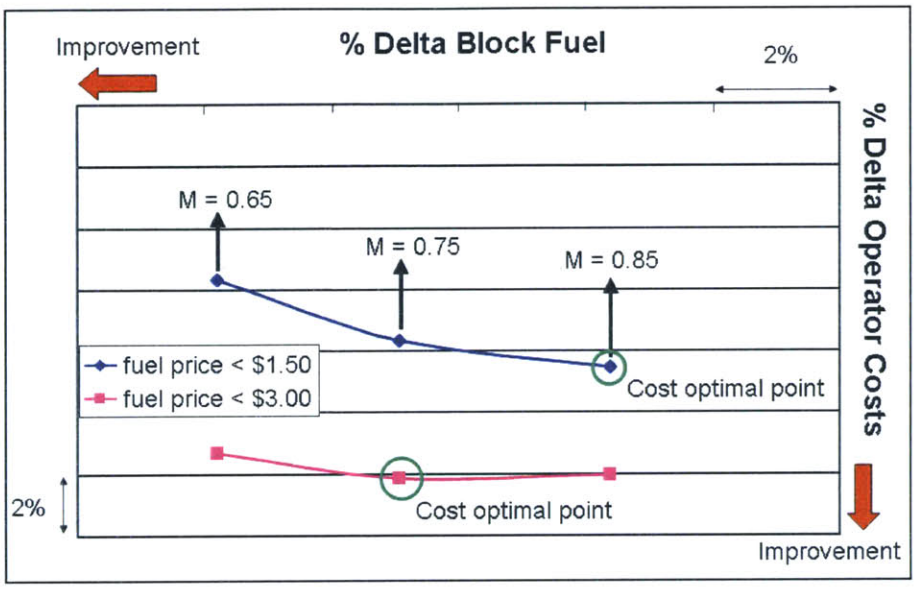

Figure 3-4: Operator costs sensitivity to cruise speed and fuel price for a fixed UEET engine

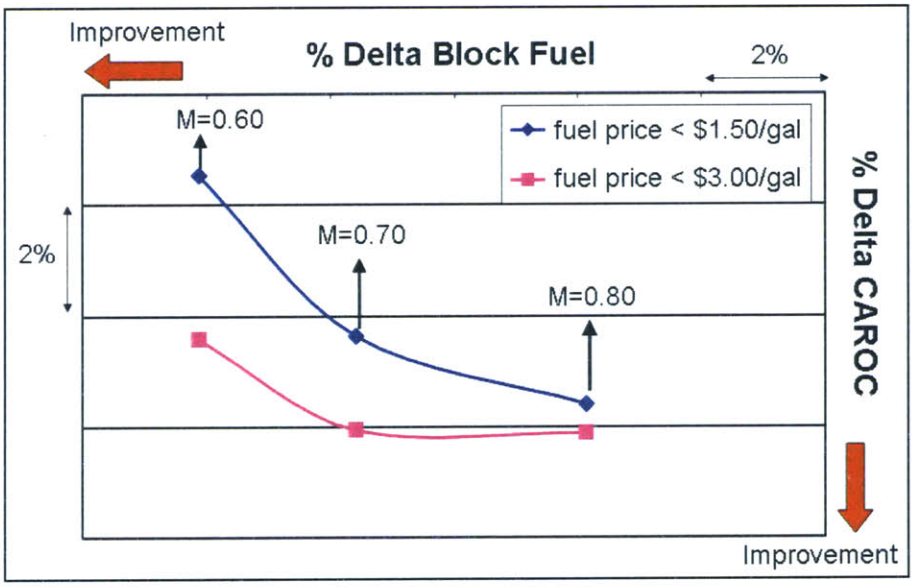

Figure 3-5: Operator costs sensitivity to cruise speed and fuel price for a fixed proprietary engine

Similar trends are noted in Figure 3-5. The cost optimal operating point for this set of engines is Mach 0.80 for both fuel prices. However, at the higher fuel price, there is a marginal change in CAROC as cruise speed is lowered to from Mach 0.80 to Mach 0.70. Given the uncertainties in the results arising from tool fidelity, the cruise Mach number 0.70 and 0.80 points at the higher fuel price may be considered as equivalent. At fuel prices higher than $3 per gallon, flying at low cruise speeds will be beneficial not only in terms of block fuel usage but also for cost savings. At high fuel prices, the driving factor in reducing operating costs will be fuel usage instead of mission block time.

Costs associated with fuel might become more crucial not only due to direct fuel price increases but also from any emissions related taxes in the future. As mentioned earlier, CO_2 values quoted from the literature range from $8 to $170 per metric tonne. Trends in fuel prices as shown in Chapter 1 also indicate further increases in fuel prices in the future. Based on these trends, the two fuel price scenarios considered here seem reasonable. From Figures 3-4and 3-5 it is important to note that approximately, for a $1.50 per gallon increase in fuel price, there is a 4% savings in fuel consumption. This value is obtained by comparing the cost optimal points indicated on both charts.

Figure 3-6 shows the same results, but expressed while keeping the fuel price fixed and varying the bypass ratio and the cruise speed. This helps in identifying the effects of varying bypass ratio on operator costs, which were not clearly captured by the previous two plots.As before, it is seen that greater cost savings are possible when flying faster for a fixed fuel price of less than $1.50 per gallon. At the high cruise speed of Mach 0.85, the medium bypass ratio is the optimum value for minimizing operator costs. This corresponds directly with the results shown in Figure 3-2, where minimum block fuel per seat is possible at a clear optimum bypass ratio value. As cruise speed decreases, Figure 3-6 shows that savings in operator costs increase with increasing bypass ratio.

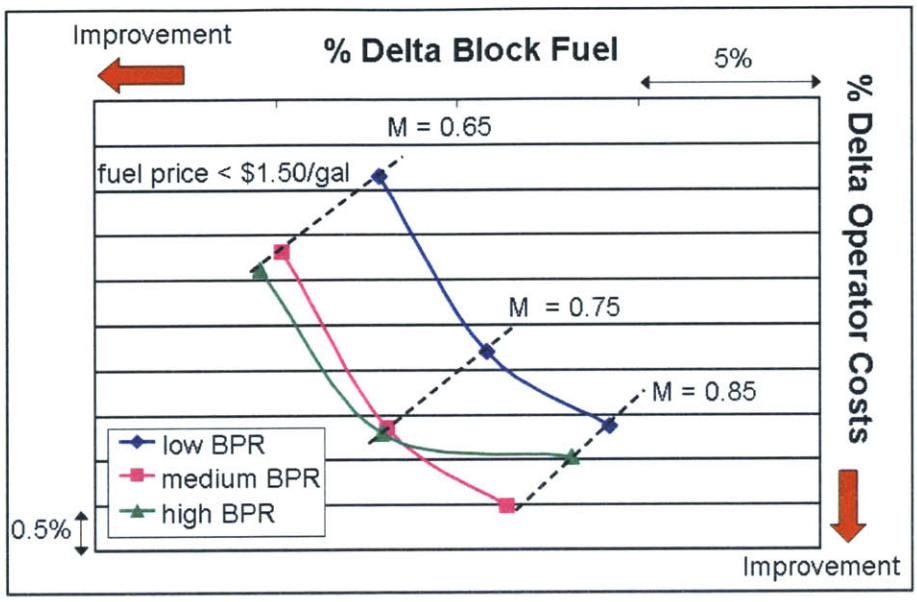

Figure 3-6: Operator costs sensitivity to cruise speed and bypass ratio for the UEET engines

For short missions, the difference in flight time caused by reducing cruise speed from Mach 0.85 to 0.65 is not as noticeable as it is for long missions. The limiting factor in deciding the optimum cruise speed for minimizing costs should also take into account utilization concerns that have not been addressed in this analysis. In reducing cruise speed and thereby increasing flight time, there may be an adverse impact on how many flights are possible per day. Additionally, as fuel prices increase significantly, this may increase other time related expenses such as crew salaries due to inflationary effects. Such a detailed economic analysis is beyond the scope of this chapter. For this study, only perturbations in fuel costs are examined, where the other components of operating costs can be assumed to remain constant. But it is important to note that such effects need to be addressed and utilization impacts need to be investigated before deciding on an optimum flight speed.

3.4 Future work recommendations

The work presented in this chapter is an initial attempt at addressing the question: what is the optimal BPR and cruise speed for a 737-sized future airplane, given

varying fuel price scenarios? As mentioned previously, initially the airplane was sized using different engines and the resulting block fuel and time data were used for an operating cost analysis. Several simplifying assumptions were made in resizing the baseline airplane for different BPRs and cruise speeds. This section critically examines these assumptions and highlights areas where further detailed analyses need to be conducted.

The assumptions made in the BPR study are fairly reasonable for a conceptual design level analysis. Since engine decks were obtained directly from manufacturers, they can be considered quite reliable as far as cycle data is concerned. One important point to be noted is that weight changes and SFC changes for optimizing engines for varying Mach number should be included in the analysis for the advanced technology engines. This was done for the UEET engines, but such data was not available for the second engine set.

With airframe redesign, the assumption that needs a critical review is that of expecting the same $M\frac{L}{D}$ performance from the airplane at different cruise speeds. Typically, cruise speed is a key design variable and wing design is centered around having an optimal configuration for a specific cruise speed that also meets other mission and performance requirements. As a first estimate, it was assumed that the wing could be reconfigured to achieve the same $M\frac{L}{D}$ performance at different cruise speeds. The next step would be to investigate how the wing needs to be changed to optimize $M\frac{L}{D}$ performance and to question if there are feasible designs such that the same performance as the baseline can be achieved at lower cruise speeds. In the following subsections, a short discussion is presented on wing design and other airplane level impacts of varying cruise speed.

3.4.1 Wing design

Wing design is the most critical analysis involved in a cruise speed study. By varying cruise speed, there are significant differences in flight aerodynamics and the wing has to be reconfigured to fly most efficiently at the required speed. Wing redesign in turn has a significant impact on performance at design conditions as well as on low

speed performance, fuel capacity, and weight and structural considerations. The most important wing design parameters for a cruise speed study are sweep, thickness to chord ratio and aspect ratio.

(i) Sweep (Λ):

Wings are traditionally sweptback due to compressibility effects. At high cruise Mach (greater than 0.6), flow over the wings enters the transonic regime and can lead to locally sonic conditions. Shock formation leads to drag and can lead to boundary layer separation and stall, depending on where the shock waves form on the wing. Wings are swept back in order to avoid the large drag rise associated with transonic flow and reduce the strength of shocks waves. Figure 3-7 shows the velocity components on a sweptback wing.

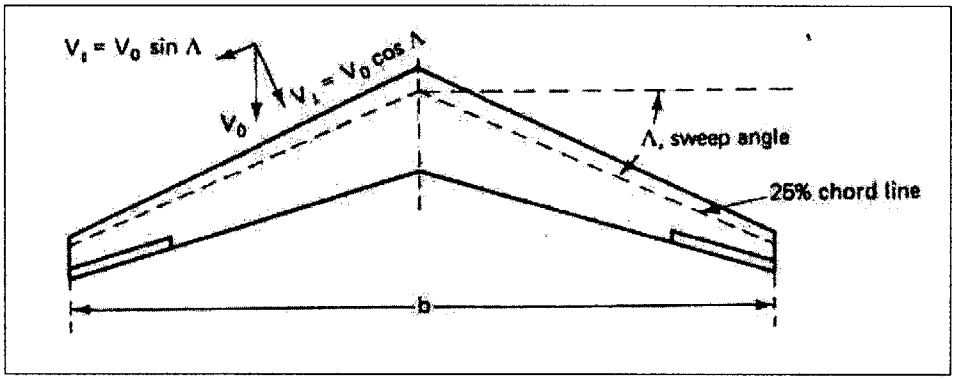

Figure 3-7: Velocity components for a sweptback wing [27]

Only the perpendicular component of the freestream velocity is important in determining flow conditions over the wing. The effective velocity and Mach seen by a sweptback wing are reduced by a factor of $\cos(\Lambda)$. Consequently, flight at higher freestream M is possible since the wing does not experience the drag rise associated with that M. However, sweep also increases wing weight due to an increased structural span and reduces C_{Lmax} [27]. When flying at lower cruise M, wing sweep can be decreased for weight reductions and improved low speed performance.

(ii) Thickness to chord ratio ($\frac{t}{c}$):

As in the case of sweep, thinner wings are generally beneficial in overcoming compressibility effects and increasing the drag divergence Mach number. Thickness to chord ratio can be increased for flying at lower speeds. The advantage in doing this lies in weight reductions and improved C_{Lmax}. Thicker wings also allow for a greater fuel volume. However, thicker wings have increased drag due to increased wetted area and separation effects. Thus, increasing thickness for lower speeds involves a tradeoff between weight and C_{Lmax} benefits versus drag penalties [27].

(iii) Aspect Ratio (AR):

Aspect ratio is defined as $\frac{b^2}{S}$ where b is the wing span and S is the wing area. AR can be increased by either reducing wing area at constant span or increasing span at constant wing area. A large wing span reduces induced drag and is desirable for good low speed performance to meet climb requirements. There are constraints on how big the span can be due to structural considerations like flutter and operational considerations like hangar or airport gate limits. Also, increasing AR causes a weight penalty and an optimum value is selected based on a tradeoff between aerodynamic and structural effects [27].

These three wing parameters are expected to be significant for a cruise speed study. Other design parameters like taper ratio, wing twist and airfoil characteristics may have secondary effects that can be explored at a more detailed design level. The wing would be reconfigured for each M_{cruise} based on the most optimum combination of the sweep, thickness to chord ratio and aspect ratio. A trade study needs to be conducted to explore the design space using these variables. Imposing constraints such as TOFL and V_{app} would then aid in sizing the airplane for the given M_{cruise} .

3.4.2 Other airplane level design changes

Based on personal communication with subject matter experts in the Boeing Company, for a first order analysis, no other structural changes are expected to be as crucial as wing design for the range of cruise speeds considered. Data from OEW

trades is shown below for the 737-sized airplane to demonstrate that other structural changes resulting in airplane weight changes will not have a significant impact on the mission block fuel performance. These trades were done by perturbing the baseline OEW and noting the trends in fuel usage. Figure 3-8 shows the results from such a study. These results are for a specific engine from the UEET set, the baseline case at M_{cruise} 0.85 is compared to cases run with changes to the airplane empty operating weight.

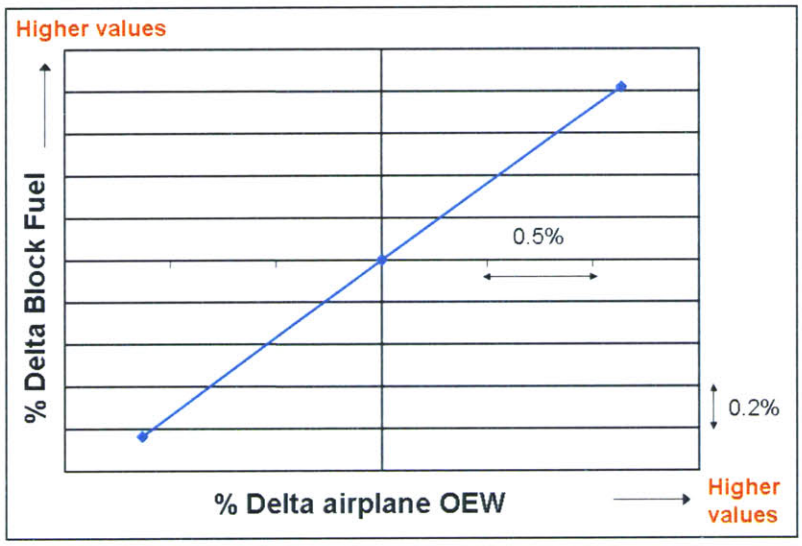

Figure 3-8: Fixed UEET engine OEW tradeoff - changes in mission block fuel

From Figure 3-8, 0.5% change in OEW leads to less than 0.4% change in block fuel usage. Thus, it can be expected that weight changes from other structural modifications will not cause a large impact on block fuel usage. Other structural changes may also add to or improve drag characteristics, but the overall effects are not expected to be large enough to radically change the results based on just a wing design.

The other important consideration was engine nacelle design for changing aerodynamic conditions. However, nacelle design is strongly driven by not only aerodynamics but also other constraints imposed by installation, engine-out requirements, accessories packages, etc. A generic answer to how nacelle design will change due to changes in cruise speed is difficult to obtain for a preliminary design study like this one. This is generally true for the cruise Mach range considered (0.60 to 0.85). When

considering higher cruise Mach numbers, drag considerations would become more significant and nacelle design would have to be taken into account for the design study. The only changes in the nacelle included in this analysis came from scaling the engine for thrust requirements. Appropriate changes in nacelle drag were included based on engine diameter correlations.

3.5 Conclusions

This analysis focused on first understanding the impacts of cruise speed and engine bypass ratio on block fuel use. Secondly, the results of the performance analyses were used to assess operator cost sensitivity to cruise speed, bypass ratio and fuel price. Two different sets of engines were used for the study and both reflected similar trends in the results. At high cruise speeds, an optimum value for the bypass ratio was noted for minimizing mission block fuel usage. However, as cruise speed was decreased the results showed that fuel use continually decreases with increasing bypass ratio for the BPR range examined. The cost sensitivity analysis showed that at a fixed bypass ratio, flying slower seemed most beneficial for high fuel prices. Also, for a fixed fuel price, operator costs were minimized at a specific value for the bypass ratio for the high cruise speeds. As the cruise speed was reduced, cost savings increased with increasing bypass ratio. A 4% savings in fuel usage was noted for an fuel price increase of approximately $ 1.50 per gallon. The purpose of this study was to demonstrate general trends in performance and in cost savings for varying bypass ratio, cruise speed and fuel price.

The assumptions used in the study were critically examined. Wing design for each distinct cruise Mach number was identified as the most important area for future work. Sweep, thickness to chord ratio and aspect ratio were the recommended as the primary wing parameters to use in a trade study. An optimum combination of these variables would define the wing configuration for flying at lower speeds. Other major airplane level structural changes were not expected to be necessary for a cruise speed study for the range of speeds considered here (cruise Mach 0.60 to 0.85). In summary,

it is important to realize that cruise speed is a critical design variable that is a driving factor in determining wing aerodynamics, engine BPR and airplane configuration. A rigorous study is necessary to understand how the wing should be best configured for different cruise flight conditions.

Chapter 4

Conclusions

This thesis consisted of two distinct studies, both with the overall aim of improving the environmental performance of future aircraft designs through technological or operational changes that should also be economically viable solutions. The first study involved the implementation of a water injection system in commercial airplane engines, which holds the potential for significant reductions in NO_x and soot emissions. Water injection reduces operating temperatures in the engine hot section and may extend engine component life. The second analysis was a trade study that looked the impacts of engine bypass ratio and cruise speed on the fuel burn and operating costs for a future 737-sized study aircraft. Operating costs sensitivity to future fuel price scenarios was also examined. This final chapter presents a brief summary and conclusions derived from the work presented and also recommends some areas for future work.

4.1 Summary and conclusions

The water injection study assessed the potential turbine blade life benefits and maintenance cost reductions due to lowered operating temperatures in the engine hot section. Low cycle fatigue, creep and oxidation were identified as the principal failure mechanisms in turbine blades. Due to the lack of proprietary data such as exact operating conditions, blade geometry, temperatures and loads, the analyses was conducted

from a purely materials perspective. Using publicly available data on representative blade materials - Inconel 625, Inconel 706 and René 80, fatigue life estimates were provided through the Universal Slopes method. The Universal Slopes method is an empirical generic approach for estimating fatigue life and is commonly used for preliminary design level analyses. For a 67K reduction in T_{t4}, a blade metal temperature reduction of up to 47K is expected. Life improvement of up to a factor of 1.90 was expected in Inconel 625, of up to 1.46 in Inconel 706 and of about 2.85 in René 80. The effects of creep and oxidation are difficult to capture in a generic manner and hence findings from a literature review were presented to demonstrate improvements in life from temperature reductions. Despite the shortcomings and limitations of the approach, it can be stated with confidence that life improvement is to be expected due to reduced operating temperatures as the result trends depicted. Also, the results were comparable in magnitude for some of the materials used to those obtained by engine companies for the Boeing study [6].

A maintenance cost analysis was also performed for the water injection study based on airline data on benefits resulting from de-rated operations. De-rate reduces operating temperatures in the turbine and so does water injection. Hence, the reduction in T_{t4} from water injection was translated into a de-rate level to extract possible maintenance cost benefits due to water injection. A 67K change in T_{t4} from water injection corresponds to de-rate values ranging from 5.1% to 11.5% depending on the engine cycle, the average value is 8.4%. For the average 8.4% de-rate value from water injection, material maintenance costs in 2004 dollars are reduced by 16.52% to 2.86% for a 1-hour and 12-hour flight length respectively. It was found that based on the engine cycle, shorter flights with more takeoffs per day had higher reductions in material maintenance costs.

Results from the water injection study were also helpful in understanding the current and future capabilities of the Environmental Design Space (EDS). EDS version 1 does not have the ability to predict engine component life and is unlikely to develop that in the future, owing to the complex and proprietary nature of the analyses required to obtain reliable results. Maintenance cost estimates are a better approach

to gauge part life benefits and the Aircraft Life-Cycle Cost Analysis Code (ALCCA) in EDS currently does that using empirical methods and historical data. Throughout the framework of EDS it will be necessary to choose appropriately between physics-based and empirical approaches depending on the complexity of the physics involved or the proprietary nature of the data needed.

The bypass ratio and cruise speed trade study for a 737-sized future airplane was done using Boeing internal tools and proprietary data. Engines with varying bypass ratios were integrated with the baseline airplane. A clear optimum in bypass ratio was found in terms of minimizing the block fuel at higher cruise speeds. For the UEET engines, the optimum BPR was about 14 when flying at cruise Mach number 0.85. At lower speeds, increasing bypass ratio continually decreased mission fuel burn. Fuel burn decreased as cruise speed was lowered.

Operating cost sensitivity to bypass ratio, cruise speed and fuel price was assessed based on the results of the trade study mentioned earlier. It was found that at low fuel prices of less than \$1.50/gallon, high cruise speeds were better in terms of operating costs due to block time effects. Flying slower was found to be most beneficial for minimizing both operating costs and fuel savings at high fuel price scenarios with fuel prices greater than \$3.00/gallon, where block fuel effects became increasingly important. The cost optimal operating points were indicated compared to the baseline for two different fuel price scenarios. A 4% reduction in fuel consumption was noted for a fuel price increase of approximately \$1.50 per gallon. This reduction resulted from flying at a lower cruise speed.

4.2 Recommendations for future work

The following suggestions are offered in terms of future areas to explore based on the studies conducted in this thesis.

Water injection and turbine durability:

- The accuracy of the Universal Slopes method can be improved if the material constants used in the equation can be experimentally obtained for the blade

material being examined.

- Better turbine life estimates can be obtained upon the availability of more material data or better models that incorporate the effects of creep and oxidation.
- Creep effects can also be included in crack propagation models to account for combined creep and fatigue effects.

Environmental Design Space:

- EDS is not likely to have engine life prediction capabilities and hence, maintenance cost estimation methods in ALCCA should be thoroughly assessed to ensure reliability of results obtained.
- EDS should consist of a combination of physics-based and empirical approaches, where an empirical method is used when good physics-based models are not available.

Bypass ratio and cruise speed trade study:

- The wing should be reconfigured with changing cruise speeds to ensure optimal performance at the given cruise speed. Detailed wing design must be pursued in the future to obtain better estimates for possible fuel burn savings from cruising slower.
- Sweep, thickness-to-chord ratio and aspect ratio are recommended as the primarily wing parameters to consider in a cruise speed study.
- While only direct operating costs were considered in this work, indirect costs - especially productivity need to be accounted to for to understand overall operational impacts of cruising slower. In other words, the question to be asked is how cruising slower would impact flight schedules and if it would results in fewer flights per day for the operator.

Appendix A

Engine cycle deck analysis for water injection: thrust-turbine inlet temperature correlations

Appendix A complements the maintenance cost estimation analysis presented in Chapter 2. Maintenance cost data was obtained from an airline for a typical 1970's technology engine showing effects of de-rated operations and flight duration. In order to extract maintenance cost estimates for water injection from this data, T_{t4} reductions from de-rated operations had to be related to changes in T_{t4} resulting from water injection. This was accomplished by plotting full throttle curves for several cycles for a single, typical 1970's technology mixed flow turbofan engine as shown below. Figures A-1 through A-5 show several different engines cycles analyzed through GasTurb [10] by varying critical parameters such as the OPR, BPR, T_{t4}, component polytropic efficiencies (η_{poly}) and the mass flow. The polytropic efficiency for each component (compressors and turbines) was kept constant at the same value and varied by the same amount while studying the impacts of polytropic efficiency on the throttle curve.

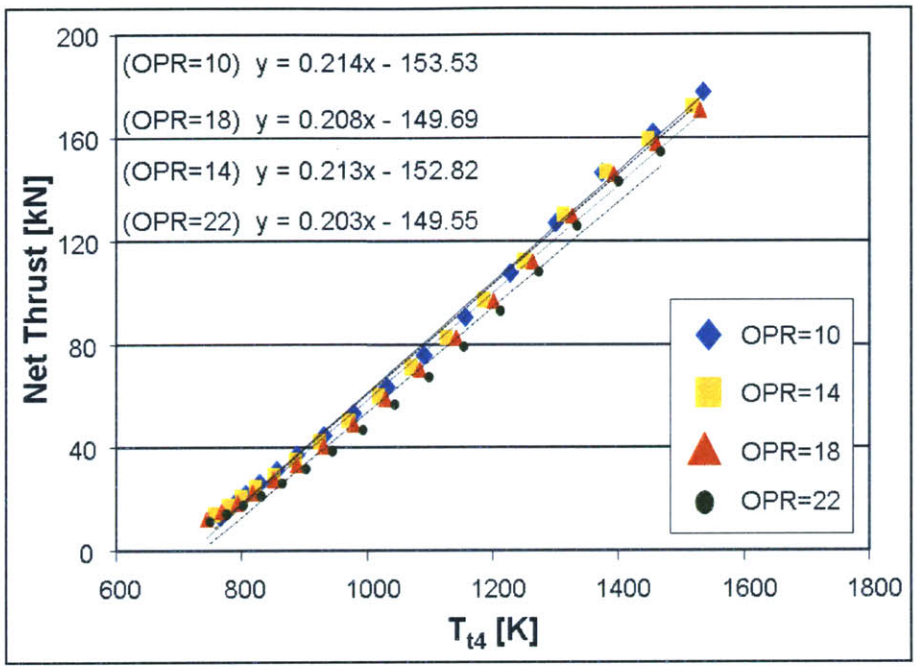

Figure A-1: Net Thrust vs. T_{t4} for varying OPR, spool speeds 0.75-1.15, Design point: BPR=4.5, $\dot{m}$=500kg/s, T_{t4}=1200K, $\eta_{poly} = 0.9$

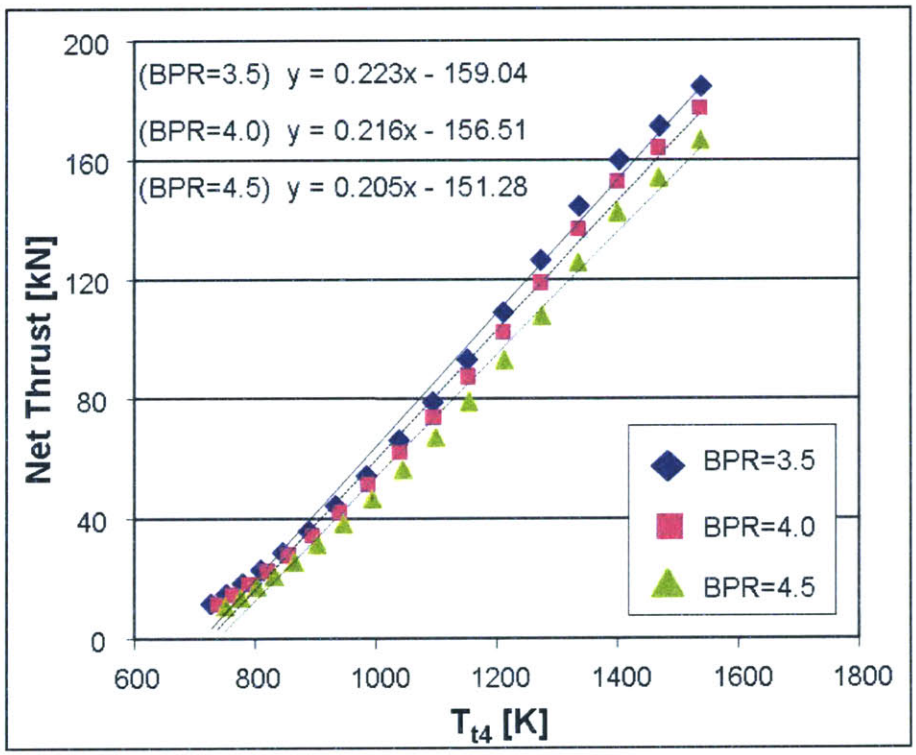

Figure A-2: Net Thrust vs. T_{t4} for varying BPR, spool speeds 0.75-1.15, Design point: OPR=22, $\dot{m}$=500kg/s, T_{t4} =1200K, $\eta_{poly} = 0.9$

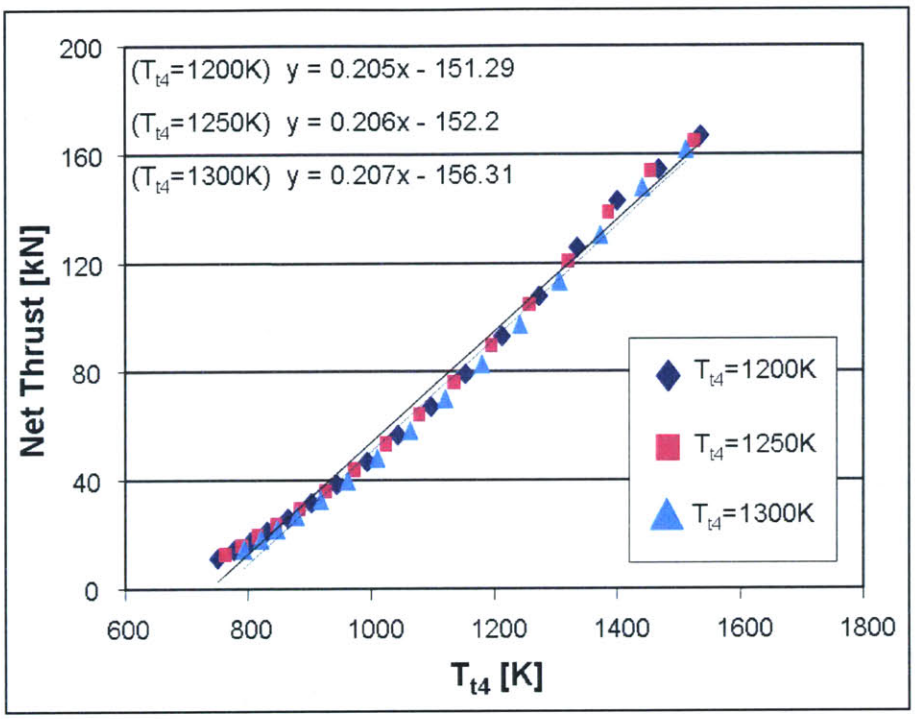

Figure A-3: Net Thrust vs. T_{t4} for varying T_{t4}, spool speeds 0.75-1.15, Design point: OPR=22, $\dot{m}$=500kg/s, BPR=4.5, $\eta_{poly} = 0.9$

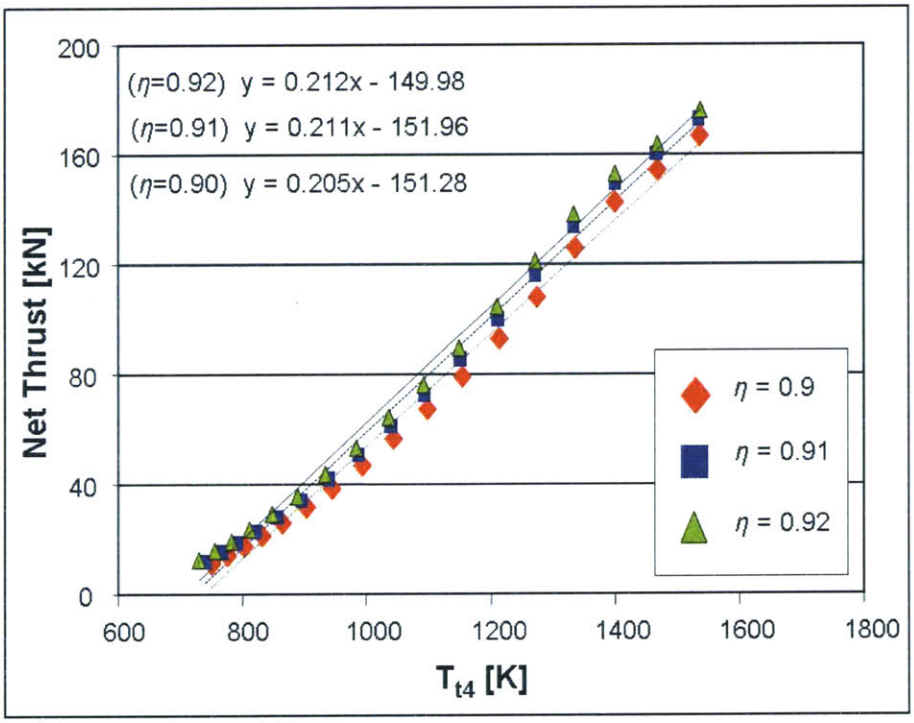

Figure A-4: Net Thrust vs. T_{t4} for varying η_{poly}, spool speeds 0.75-1.15, Design point: OPR=22, $\dot{m}$=500kg/s, BPR=4.5, T_{t4} =1200K

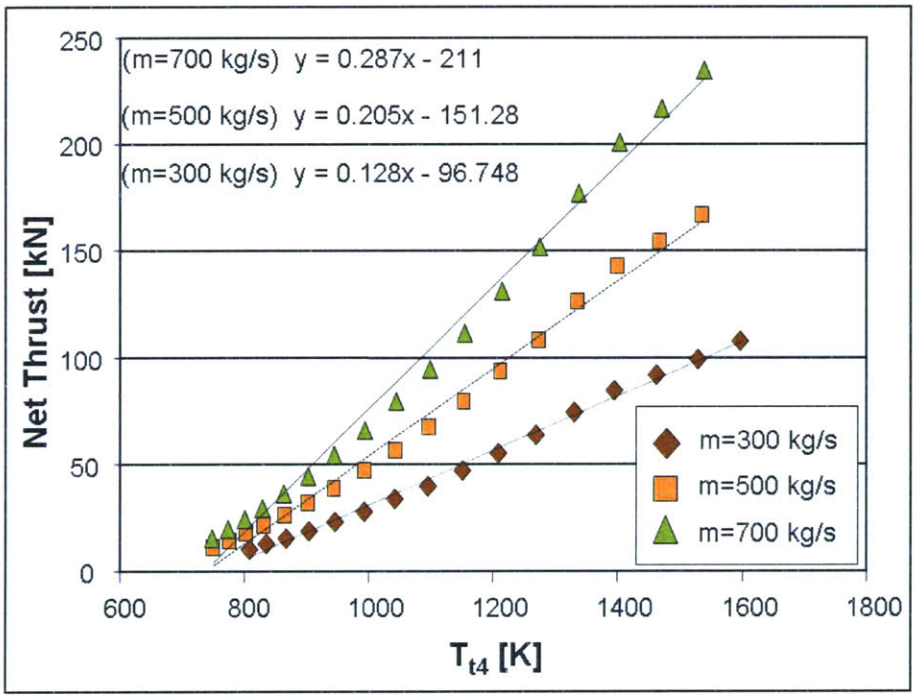

Figure A-5: Net Thrust vs. T_{t4} for varying mass flow, spool speeds 0.75-1.15, Design point: OPR=22, BPR=4.5, T_{t4} =1200K, $\eta_{poly} = 0.90$

Appendix B

Turbine blade heat transfer analysis

It has been mentioned earlier in Chapter 2 that changes in turbine inlet gas temperature do not have a 1:1 correspondence with blade metal temperature. Blade life impacts were presented for a range of metal temperature changes determined based on personal communication with Boeing. For more accurate estimates, a blade heat transfer analysis is recommended. Appendix B presents a brief overview of the heat transfer mechanisms involved. The purpose of this analysis is to demonstrate how changes in T_{t4} can be correlated to changes in blade metal temperature.

For air-cooled turbines, there are three principal mechanisms of heat transfer: convection from external gas flow to the external wall, conduction through through the blade metal and finally convection from internal blade walls to the cooling flow. The effects of film cooling and blade protective coatings are not considered here. Details like cooling flow path and mechanisms are also omitted for simplicity and to present the physics involved for a first order approximation. The analysis presented is based on class notes from an MIT Aeronautics and Astronautics course [28].

The external convection heat transfer is given by:

$$\dot{q}_{ext} = h_{ext}(T_{gas} - T_{w,o}) \tag{B.1}$$

$\dot{q}_{ext}$ = external heat transfer rate [W/m^2]

h_{ext} = external heat transfer coefficient [W/m^{2}K]

T_{gas} = turbine inlet external gas temperature [K]

$T_{w,o}$ = blade outer wall metal temperature [K]

The conduction heat transfer in the blade is:

$$\dot{q}_{wall} = \frac{k}{t}(T_{w,o} - T_{w,i}) \tag{B.2}$$

$\dot{q}_{wall}$ = wall conduction heat transfer rate [W/m^2]

k = wall thermal conductivity [W/mK]

t = wall thickness [m]

$T_{w,i}$ = blade inner wall metal temperature [K]

Finally, the inner blade wall convection heat transfer is:

$$\dot{q}_{int} = h_{int}(T_{w,o} - T_{cool}) \tag{B.3}$$

$\dot{q}_{int}$ = external heat transfer rate [W/m^2]

h_{int} = external heat transfer coefficient [W/m^{2}K]

T_{cool} = cooling flow gas temperature [K]

Assuming a steady state thermal balance, external convection heat transfer to the blade must equal conduction within the blade and convection heat transfer from the internal surface to the cooling flow:

$$\dot{q}_{ext} = \dot{q}_{wall} = \dot{q}_{int} \tag{B.4}$$

Water injection in the engine combustor impacts turbine inlet temperature and does not alter cooling flow temperatures to a first degree approximation. Hence, the average wall temperature, $T_{wall,1}$ can be determined by equating the internal

and external convection heat transfers. The subscript '1' denotes baseline conditions without water injection.

$$h_{ext,1}(T_{gas,1} - T_{wall,1}) = h_{int,1}(T_{wall,1} - T_{cool}) \tag{B.5a}$$

$$T_{wall,1} = \left(\frac{h_{ext,1}}{h_{ext,1} + h_{int,1}}\right) T_{gas,1} + \left(\frac{h_{int,1}}{h_{ext,1} + h_{int,1}}\right) T_{cool} \tag{B.5b}$$

Water injection reduces turbine inlet temperature and the new gas temperature is $T_{gas,1} - \Delta T_{gas}$. The subscript '2' denoted modified values due to external gas temperature change. The new average wall temperature due to this change is:

$$T_{wall,2} = \left(\frac{h_{ext,2}}{h_{ext,2} + h_{int,2}}\right) (T_{gas,1} - \Delta T_{gas}) + \left(\frac{h_{int,2}}{h_{ext,2} + h_{int,2}}\right) T_{cool} \tag{B.6}$$

Finally the change in wall temperature caused by the change in external gas temperature can be expressed as $\Delta T_{wall} = T_{wall,1} - T_{wall,2}$. Assuming that the internal and external wall heat transfer coefficients remain constant, the change in wall temperature is:

$$\Delta T_{wall} = \left(\frac{h_{ext}}{h_{ext} + h_{int}}\right) \Delta T_{gas} \tag{B.7}$$

ΔT_{wall} can then be estimated depending on the availability of data on heat transfer coefficients.

Bibliography

[1] Boeing, Current Market Outlook 2005, The Boeing Company, Seattle, United States, 2005

[2] Federal Aviation Administration, "FAA Aerospace Forecasts Fiscal Years 2006-2017," Office of Aviation Policy and Plans, U.S. Department of Transportation, 2006.

[3] Lee, J.J., Lukachko, S.P., Waitz, I.A., "Aircraft and Energy Use," invited chapter in the *Encyclopedia of Energy, Volume 1*, by Academic Press/Elsevier Science, San Diego, California, March 2004.

[4] Waitz, I.A., Townsend, J., Cutcher-Gershenfeld, J., Greitzer, E.M., Kerrebrock, J.L., "Aviation and the Environment: A National Vision Statement, Framework for Goals and Recommended Actions," Report to the United States Congress, on behalf of the U.S. DOT, FAA and NASA, December 2004 (delivered to Congress December 2005).

[5] Partnership for AiR Transportation Noise and Emissions Reduction (PARTNER), "Architecture Study for the Aviation Environmental Portfolio Management Tool (APMT)," An FAA/NASA/Transport Canada-sponsored Center of Excellence, 2006.

[6] Daggett, D.D., Hendricks, R.C., Mahashabde, A., Waitz, I.A., "Water injection could it reduce airplane maintenance costs and airport emissions?," ISABE-2005-1249, 17th International Symposium on Airbreathing Engines, Munich, Germany, September 4-9,2005.

[7] Bureau of Transportation Statistics, "Transportation Statistics Annual Report," Research and Innovative Technology Administration, U.S. Department of Transportation, November, 2005.

[8] Intergovernmental Panel on Climate Change, *Aviation and the Global Atmosphere.* 1999: Cambridge University Press, USA, http://www.grida.no/climate/ipcc/aviation/index.htm

[9] Dings, J.M.W., Wit, R.C.N., Leurs, B.A., Davidson, M.D., Fransen, W., "External costs of aviation," Umweltbundesamt, Germany, 2002.

[10] Kurzke, J., "GasTurb 9," www.gasturb.de

[11] Personal communication with an airline.

[12] Daggett, D.L., Water Injection Feasibility for Boeing 747 Aircraft, NASA CR 2005-213656, 2005.

[13] Suresh, S., *Fatigue of materials.* 2nd ed. 1998: Cambridge University Press, MA.

[14] Manson, S.S., "Fatigue: A Complex Subject - Some Simple Approximations," The William M. Murray Lecture, 1964, Presented at 1964 SESA Meeting,Cleveland, Ohio, 28-30 October.

[15] High Temp Metals Inc., Technical library, http://www.hightempmetals.com/technicaldata.php

[16] Military Handbook - MIL-HDBK-5H: Metallic Materials and Elements for Aerospace Vehicle Structures, 2003 U.S. Department of Defense.

[17] Klopp, W.D., Nonferrous alloys, Aerospace Structural Metals Handbook, Code 4214, pp 1-18, Sept 1984.

[18] Zupnik, T.F., "Hot Section Technology," Pratt Whitney, GTL Lecture Series-MIT, 1979.

[19] Li, S.X., and Smith, D.J., "High Temperature fatigue-creep crack initiation and propagation of a single crystal nickel base superalloy," IMechE Conference Transactions: Creep and Fatigue, pp 279-288, April 1996.

[20] Newell, J.F., "A Note of Appreciation for the MUS," Material Durability/Life Prediction Modeling: Materials for the 21st Century, PVP-290, ASME, New York, pp. 5758, 1994.

[21] Lee J.J., *Modeling Aviation's Global Emissions, Uncertainty Analysis, and Applications to Policy*, PhD Thesis, Massachusetts Institute of Technology, February 2005.

[22] Gamache, B., "Emerging Trends in Aircraft Engine Maintenance and Services," Pratt Whitney.

[23] Georgia Institute of Technology, "Aircraft Life Cycle Cost Analysis (ALCCA) version 6.0," Aerospace Systems Design Laboratory, Atlanta, GA, 2001.

[24] Daggett, D.L., Brown, S.T., Kawai, R.T., Ultra-Efficient Engine Diameter Study, NASA CR 2003-212309, May 2003.

[25] Padilla, C.E., *Optimizing Jet Transport Efficiency.* 1996: McGraw-Hill Companies, Inc., NY.

[26] Antoine, N.E., *Aircraft Optimization for Minimal Environmental Impact*, PhD Thesis, Stanford University, August 2004.

[27] Shevell, R.S., *Fundamentals of Flight.* 2nd ed. 1989: Prentice Hall Inc., New Jersey.

[28] Epstein, A.H., "Turbine Durability, Heat Transfer and Cooling," Lecture notes, MIT Course 16.511 - Aircraft Engines and Gas Turbines, 2004.